Biological Sciences Faculty Publications

Faculty Publications

10-8-2024

Crocodylian diversity during the early Eocene climatic optimum in the Golden Valley Formation of North Dakota, U.S.A.

Adam P. Cossette
New York Institute of Technology

David Tarailo
Fort Hays State University, datarailo@fhsu.edu

Follow this and additional works at: https://scholars.fhsu.edu/biology_facpubs

Part of the Biology Commons

Crocodylian diversity during the early Eocene climatic optimum in the Golden Valley Formation of North Dakota, U.S.A.

Adam P. Cossette & David A. Tarailo

View supplementary material ⧉

Published online: 08 Oct 2024.

Submit your article to this journal ⧉

Article views: 760

View related articles ⧉

View Crossmark data ⧉

Check for updates

ARTICLE

CROCODYLIAN DIVERSITY DURING THE EARLY EOCENE CLIMATIC OPTIMUM IN THE GOLDEN VALLEY FORMATION OF NORTH DAKOTA, U.S.A.

ADAM P. COSSETTE, [1,*] and DAVID A. TARAILO[2]

[1]Department of Biomedical & Anatomical Sciences, New York Institute of Technology College of Osteopathic Medicine at Arkansas State University, Jonesboro, Arkansas 72401, U.S.A., acossett@nyit.edu;
[2]Department of Biological Sciences, Fort Hays State University, Hays, Kansas 67601, U.S.A.

ABSTRACT—Rich bone beds from the lower Eocene strata of the Golden Valley Formation of Stark County, North Dakota reveal a speciose sympatric crocodylian fauna. However, analyses demonstrate limited phylogenetic diversity among these co-occurring taxa, and of the four species known for the locality, three are alligatorids and one is a crocodyloid. Phylogenetic hypotheses recover *Chrysochampsa mylnarskii* as a late lived member of Brachychampsini—a stem-based clade including *Brachychampsa montana* and all alligatorids more closely related to it than to *Caiman crocodilus* or *Alligator mississippiensis*—and a new genus and species, *Ahdeskatanka russlanddeutsche* groups with species of *Allognathosuchus*. The crocodylians, partitioned by body size and plan, would have occupied an array of ecological niches and feeding strategies. Whereas the large-bodied alligatorid *Chrysochampsa mylnarskii* preserves a generalist morphology, *Ahdeskatanka russlanddeutsche* bears a short, broad snout and globular distal teeth. Contemporaneous with a peak in alligatoroid diversity during this interval, *Ahdeskatanka russlanddeutsche* is an exemplar of a radiation of small-bodied alligatorids with crushing dentition and preserves the ancestral alligatorid feeding strategy. Trophic dynamics of the locality diverge from modern environments and the abundant crocodylians may have filled the ecological niche of large mammalian carnivores conspicuously absent here. This alligatorid-rich crocodylian fauna evolved in swampy lowlands and meandering streams flanked by subtropical forests during one of the hottest sustained intervals in Earth history. The lush, highly productive ecosystems preserved in the Golden Valley Formation inform the evolutionary history of North American alligatorids and preserve significant biodiversity following the Paleocene–Eocene Thermal Maximum.

INTRODUCTION

Crocodylia is a reptile clade that includes the last common ancestor of *Gavialis gangeticus*, *Alligator mississipiensis*, *Crocodylus niloticus*, and all of its descendants (Brochu, 2003). Modern crocodylians are semiaquatic apex predators with low morphological diversity and a tropically restricted geographic range. However, the crocodylian fossil record reveals extraordinary biodiversity, broad latitudinal distribution, disparate body sizes and bauplans, and the occupation of numerous ecological niches and feeding strategies (Brochu, 1999, 2001). Analysis of modern crocodylian ranges indicates that temperature is a key driver of their distribution with standing water acting as a thermal buffer against extreme temperatures (Marckwick, 1998) and the paleodistribution of fossil crocodylians matches patterns seen with modern populations (De Celis et al., 2020; Mannion et al., 2015; Solórzano et al., 2020).

The Golden Valley Formation of North Dakota, U.S.A. preserves exposures of the Paleocene–Eocene Thermal Maximum (PETM) and the following Early Eocene Climatic Optimum (EECO) (Murphy, 2009). This brief but prominent period of warming occurred in response to a global increase in carbon dioxide. Studies show global surface temperatures increased by about 6° Celsius from the late Paleocene through early Eocene and summer surface air temperatures near 40° Celsius are predicted for the study region (McInerney & Wing, 2011; Tierney et al., 2022). Following this thermal maximum event, the Golden Valley Formation preserves sediments concurrent with the EECO, representing one of the hottest sustained intervals in Earth history (Scotese et al., 2021). Intense global warming

over this interval is associated with changing environments, increased habitat complexity in terrestrial biomes, floral diversification, and the greatest episode of faunal turnover in the early Cenozoic (Woodburne et al., 2009).

Western North Dakota during the latest Paleocene—earliest Eocene was warm and humid, dominated by swamps and marshes with dense subtropical forests along sinuous rivers and streams (Hickey, 1977). Regional paleohydrology was intensely variable during this interval (Clechenko et al., 2007) and these processes deposited the sedimentary complexes of the Golden Valley Formation during the progressive infilling of the Williston Basin. Yet, floral communities were stable and palynology indicates little change in composition across the Paleocene–Eocene boundary (Harrington et al., 2005). In this environment a diverse fauna existed, dominated by riparian and aquatic taxa including freshwater and terrestrial invertebrates, mammals, fish, salamanders, anurans, turtles, lizards, and four or five species of crocodylians (Estes, 1988; Hickey, 1977; Jepsen, 1963).

Concomitant with this warm period was a spike in North American alligatorid diversity (De Celis et al., 2020), evidence of which is preserved in sediments of the Golden Valley Formation. These taxa dominate the crocodylian fauna of the lower Eocene Camels Butte Member of the Golden Valley Formation and the assemblage is remarkable in representing one of the most taxonomically diverse crocodylian localities, while representing limited morphological and phylogenetic diversity. Zeniths of sympatric crocodylian diversity from other formations are based on fossils from many locations correlated between multiple horizons rather than sourcing from a single locality (Cozzuol, 2006; Scheyer et al., 2013).

The Golden Valley Formation has produced considerable data coupling the evolutionary and ecological record of the Paleogene age North American alligatorid diversity peak. This manuscript as part of a larger project describes the crocodylian taxa of the Golden Valley Formation at two closely spaced sites within a single locality and interval. Efforts to describe crocodylian specimens from the locality have been limited prior to this work and the authors seek to elucidate the trophic dynamics of the locality and determine the phylogenetic relationships of this endemic and highly diverse crocodylian community.

GEOLOGICAL SETTING

The Golden Valley Formation is exposed as erosional remnants scattered across the prairie landscape in the Williston Basin of North Dakota. Benson and Laird (1947) applied the name Golden Valley Formation to rocks in western North Dakota, deriving the formational name from outcrops near the town of Golden Valley in western Mercer County (Fig. 1). Benson (1949, 1953) divided the stratigraphy of the Golden Valley Formation into upper and lower members (Fig. 2). These members were further described and formalized by Hickey (1967, 1977), who named the lower, brightly colored claystone the Bear Den Member (the Hebron Member of Hickey [1967]) and the overlying unit the Camels Butte Member (the Dickenson Member of Hickey [1967]).

The Bear Den Member conformably overlies the Sentinel Butte Formation of the Fort Union Group (Fig. 2), and all evidence suggests continuous deposition across the lower boundary of the Golden Valley Formation. Lithology of the Bear Den Member, dominated by mudstone and claystone, also consists of kaolinitic sandstone and siltstone. In outcrop, this member
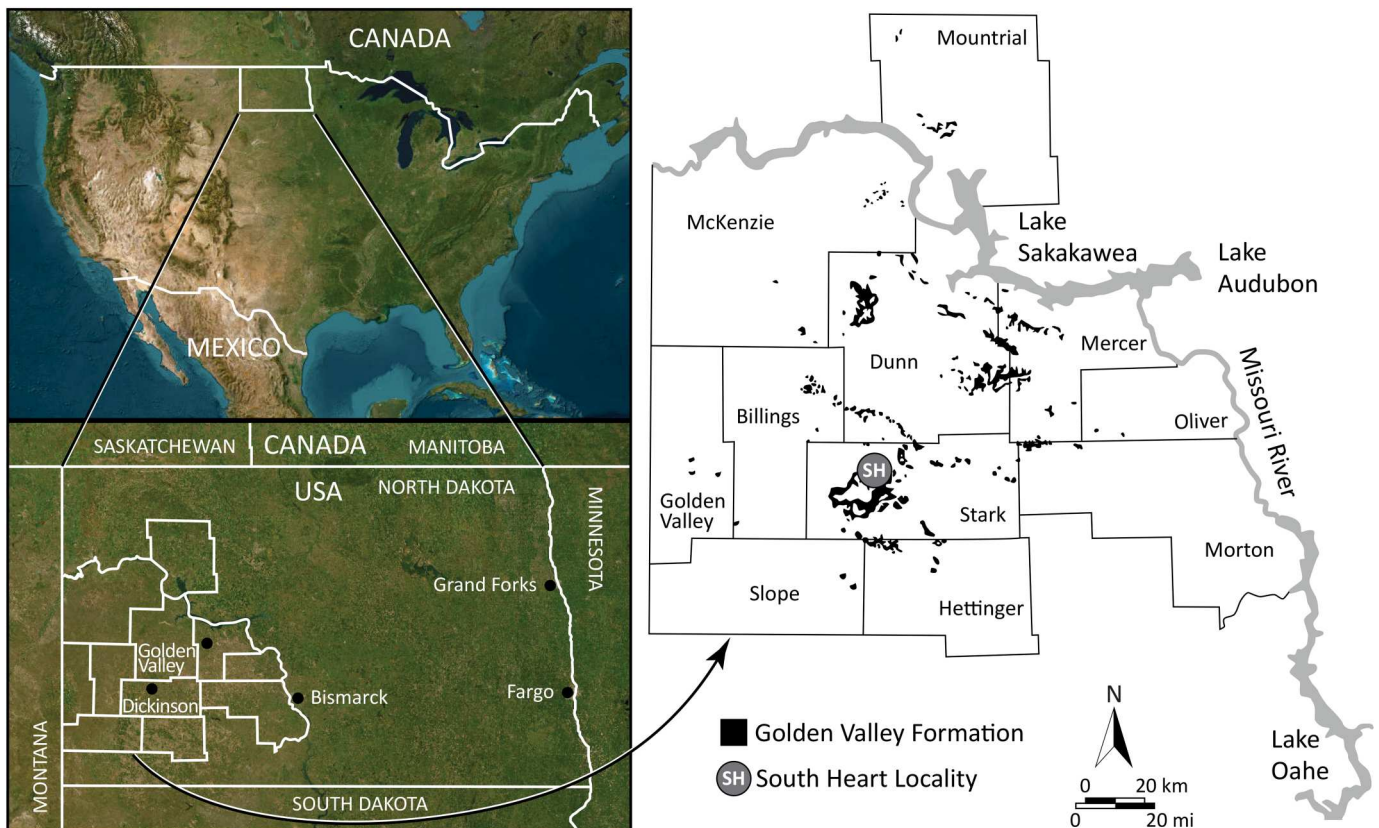

FIGURE 1. Map demonstrating position of North Dakota, U.S.A. (top left); location of counties in western North Dakota (bottom left); known outcrops of the Golden Valley Formation (after Murphy, 2009) and position of the South Heart Locality (right).
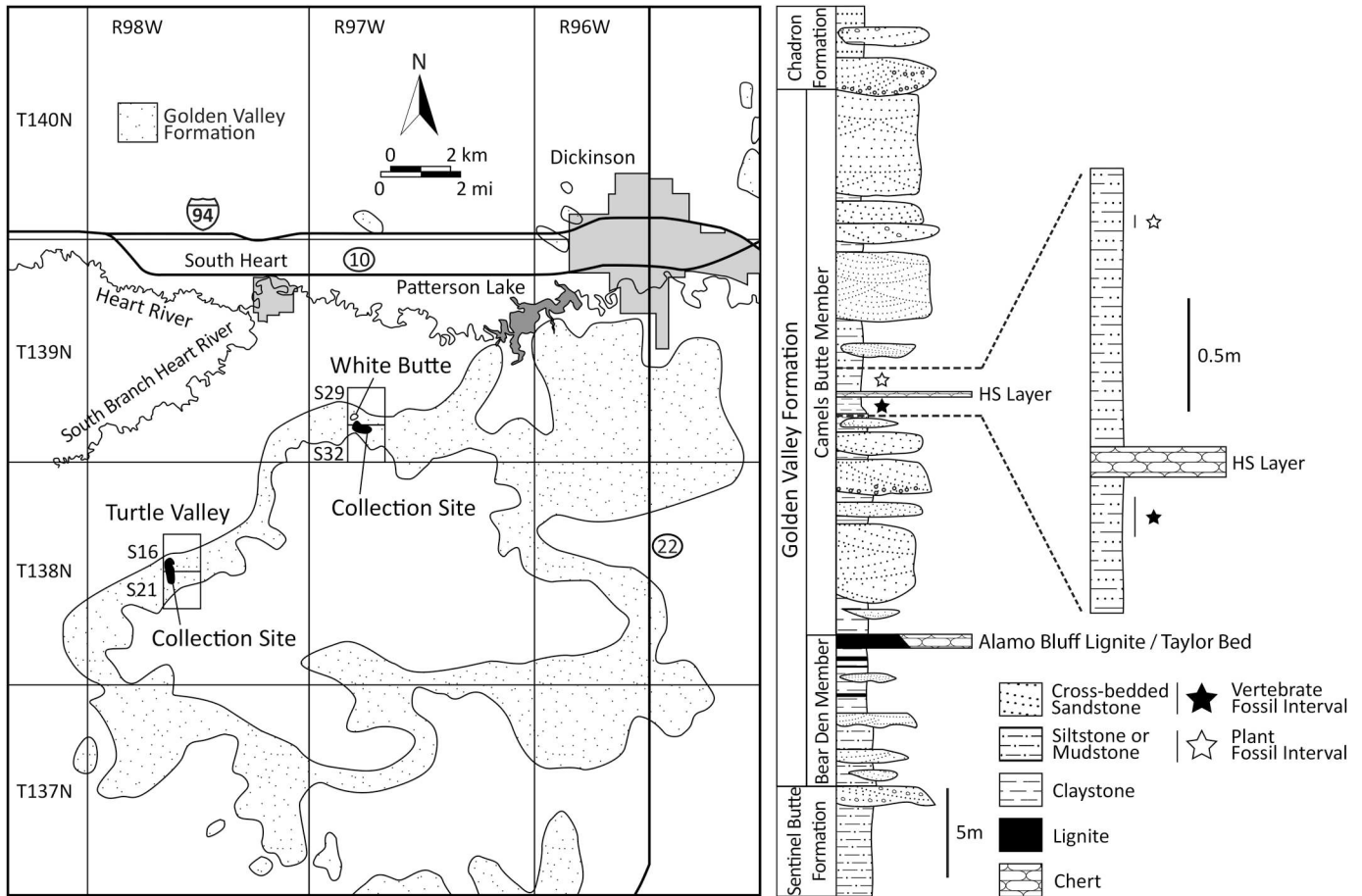
FIGURE 2. Map of Golden Valley Formation outcrops and fossil collection sites near South Heart and Dickinson, Stark County, North Dakota, U.S.A. (left). Modified and updated from Jepson (1963) to reflect subsequent changes in physical and human geography. Stratigraphic column of the Golden Valley Formation at the South Heart Locality (right). **Abbreviation**: **HS**, hard siliceous.

bears a tripartite color zonation made up of a gray zone at the base, a middle orange zone, and a brownish–orange zone near the top. The striking colors of the Bear Den Member come from well-developed paleosols formed in a warm and humid environment spanning the PETM (Murphy, 2009; Murphy et al., 2023). The member becomes increasingly fine-grained upsection, and is topped by a thin lignite layer (the Alamo Bluff lignite) in most localities, but this laterally grades into a siliceous layer (the Taylor Bed) found in others (Hickey, 1977). This trend toward decreased grain size has been interpreted as resulting from a decreased availability of clastic sediment due to changes in regional tectonics, and a shift to a lower-energy fluvial setting (Hickey, 1967) allowing for a greater frequency of standing water. Diagenesis of a peat-like soil crust, as indicated by numerous fossil plant stem molds, has been proposed as a mechanistic explanation for the siliceous Taylor Bed (Hickey, 1977).

Within the formation, the Camels Butte Member conformably overlies the Bear Den Member (Fig. 2) (Hickey, 1977). The Camels Butte Member is substantially thicker than the Bear Den Member (up to 105 meters in thickness compared with 15 meters) and consists of alternating yellow/brown cross-bedded sandstone, siltstone, mudstone, claystone, and thin lignites. These strata are interpreted as sandy channel deposits cutting into parallel-bedded, fine-grained floodplain deposits (Hickey, 1977). The proportion of channel deposits increases toward the middle and upper parts of the member

with thick and massive channel sandstones predominating many exposures, representing increasing fluvial energy and a greater occurrence of channel scouring. Vertebrate fossils and the index fossil fern *Salvinia preauriculata* indicate an early Eocene age for this upper member (Hickey, 1977; Murphy et al., 2023). The Camels Butte Member is truncated by an unconformity that marks the lower boundary of the Chadron Formation of the White River Group (Hickey, 1977; Keroher, 1966; Murphy, 2009).

Age estimates for the formation's strata evolved over a period of decades. Initially the entire formation was considered to be Eocene in age (Benson & Laird, 1947), but Hickey (1977) later refined this estimate by distinguishing the uppermost Paleocene Bear Den Member from the lower Eocene Camels Butte Member. Current estimates indicate a depositional age of 50–57 million years ago for the formation as a whole (Murphy, 2009). Palynological and carbon isotope ratios suggest a terrestrial record of the PETM at the top of the Bear Den Member, and the EECO in the overlying Camels Butte Member (Clechenko et al., 2007; Harrington et al., 2005; Murphy et al., 2023).

Vertebrate fossils are known primarily from the Camels Butte Member. The terrestrial vertebrate fossil assemblage indicates a close association between the fauna of the Golden Valley Formation and numerous lower Eocene sedimentary units including the following: rocks of the Grey Bull beds (lower Wasatchian) of the lower Willwood Formation of the Bighorn Basin of

Wyoming; the Kingsbury Conglomerate Member of the Wasatch Formation of the Powder River basin of Wyoming; the Wasatch strata of the Bearpaw Mountain locality of Montana; the Red Desert Tongue and Knight Member of the Wasatch Formation of Wyoming; and the Hiawatha Member of the Wasatch Formation in the Sand Wash basin of Colorado (Gazin, 1962; Jepsen, 1963; McKenna, 1960; Pipiringos, 1955). The eutherian genera *Homogalax, Lophiparamys, Palaeictops, Pelycodus, Reithroparamys, Teilhardina,* and *Tetonoides*, as well as the multituberculate relic *Parectypodus,* are all indicative of the lower Eocene Wasatchian NALMA (Janis et al., 1998, 2008; Jepsen, 1963). Additional mammalian taxa from the unit include *Didymictis, Hyopsodus, Paramys,* and *Sinopa*. The Camels Butte Member is regarded as belonging to the Wa3 NALMA subdivision by both Woodburne (2004) and Janis et al. (2008), the age of which is estimated by Woodburne (2004) to be between 53–55 Ma.

The formation's non-mammalian vertebrate fauna also comes primarily from the Camels Butte Member and was thoroughly cataloged by Estes (1988). This community includes fish represented by species of *Amia, Atractosteus,* and various indeterminable teleosts; amphibians including species of the salamanders *Batrachosauroides* and *Chrysoriton* and indeterminate species of anurans; turtles such as *Baptemys, Echmatemys, Plastomenus,* and *Trionyx*; lizards represented by species of *Xestops, Saniwa, Peltosaurus,* and glyptosaurids; and crocodylians represented by a number of genera (Estes, 1988; Hickey, 1977; Jepsen, 1963). The Camels Butte Member also preserves invertebrate fossils including freshwater mollusks and a species of ground-dwelling crabid beetle (Hickey, 1977; Jepsen, 1963).

Riparian and aquatic plants dominate the Bear Den Member floral assemblage. Biofacies indicate humid lowland swamps and poorly drained floodplains inhabited by subtropical forests along slow-moving streams (Hickey, 1977; Jepsen, 1963). Leaf analysis by Hickey (1977) indicates a Bear Den Member megaflora consisting of 41 species including both floating and rooted aquatic plants, as well as lowland forest species represented by ferns, conifers, and dicots closely resembling the upper Paleocene fossil flora of the Fort Union Group (Hickey, 1977).

Plant species commonly associated with Eocene ecosystems, including the index fossil *Salvinia preauriculata*, first appear in the lignite and siliceous layers capping the Bear Den Member and gradually replace Paleocene species upsection through the lower portions of the Camels Butte Member. The floral assemblage of 37 species found in the upper parts of the member has little in common with communities described from other Paleogene formations (Hickey, 1977). An upsection shift in biofacies is indicated by a reduction in the distribution and abundance of swamp and aquatic vegetation with lowland subtropical forest species becoming numerically well represented (Hickey, 1977).

As indicated by the fossil flora and fauna, palynological, and carbon isotope evidence, the climate was warm throughout the period of deposition but varied among the members. Climatic conditions during the upper Paleocene deposition of the Bear Den Member were warm and moderate with mean annual temperature estimated to be 15° Celsius (Hickey, 1977). Climate became increasingly warm and subtropical across the Paleocene/Eocene boundary and during the early Eocene deposition of the Camels Butte Member with estimated mean annual temperatures of 18.5° Celsius through this interval (Hickey, 1977). Comparison to the modern mean annual temperature of 5.6° Celsius for Dickinson, North Dakota (Western Regional Climate Center, 2016) reveals a starkly contrasting paleoclimate.

HISTORY OF THE LOCALITY

During the summers of 1958–1961, the largest field research project to date exploring the Golden Valley Formation occurred in two locations southeast and southwest of South Heart, Stark County, North Dakota, U.S.A. (Figs. 1, 2). A large expedition, led by Glenn Jepsen of Princeton University engaged in surface prospecting and quarrying in the Little Badlands Basin within the larger Williston Basin. This effort, included as part of a larger project, assessed the age of the formation and made correlations to other fossil-bearing strata in the wider region. Initial identification noted 39 species of vertebrates including a diverse crocodylian fauna present at the locality (Jepsen, 1963). Richard Estes identified many of the reptile fossils collected during this period and later (Estes, 1988) returned to work on the fauna, setting the foundation for the study here.

The White Butte (SW ¼ section 29 and NW ¼ section 32, T139NR97W) and Turtle Valley (SW ¼ section 16 and NW ¼ section 21, T138NR98W) sites are located south of South Heart, Stark County, North Dakota and collectively referred to here on as the South Heart Locality which encompasses both sites (Figs. 1, 2). A topographically prominent erosional feature within a few hundred meters of the collection site, and the preponderance of turtle fossils found, give each location their respective names. These sites, separated by a distance of 11 km produced several hundred identifiable vertebrate fossils, along with several thousand unidentifiable fragments recovered via both quarry and surface collection methods (Estes, 1988; Jepsen, 1963). The vertebrate fossils, along with a large assemblage of fossil leaves and coprolites (some of which are attributed to crocodylians), were collected from the upper member of the formation, whereas only unidentifiable bone fragments were found in the lower member (Jepsen, 1963) and are not discussed here. The most fossiliferous layers are found within close proximity of a hard siliceous (HS) layer, with most vertebrate fossils coming from a few tens of centimeters below the HS layer, and the majority of plant fossils from a very rich leafy layer about 1 meter stratigraphically above the HS layer (Fig. 2) (Hickey, 1967).

Institutional Abbreviations—**AMNH**, American Museum of Natural History, New York, New York, U.S.A.; **CM**, Carnegie Museum of Natural History, Pittsburgh, Pennsylvania, U.S.A.; **MNHN**, Muséum National d'Histoire Naturelle, Paris, France; **USNM**, United States National Museum, Washington, D.C., U.S.A.; **YPM VPPU**, Yale Peabody Museum Princeton University Vertebrate Paleontology Collection, New Haven, CT, U.S.A.

Anatomical Abbreviations—**alp**, anterolateral process; **alv**, alveoli; **an**, angular; **bo**, basioccipital; **bs**, basisphenoid; **CN**, cranial nerve; **cr**, cranioquadrate recess; **d**, dentary; **ect**, ectopterygoid; **emf**, external mandibular fenestra; **ena**, external narial aperture; **eo**, exoccipital; **f**, frontal; **fic**, foramen intermandibularis caudalis; **fm**, foramen magnum; **gf**, glenoid fossa; **if**, incisive foramen; **itf**, infratemporal fenestra; **j**, jugal; **jp**, jugal process; **l**, lacrimal; **lf**, lingual foramen; **mx**, maxilla; **mg**, Meckelian groove; **ms**, mandibular symphysis; **n**, nasal; **oa**, otic aperture; **orb**, orbit; **pa**, parietal; **pal**, palatine; **pf**, prefrontal; **pmx**, premaxilla; **po**, postorbital; **pt**, pterygoid; **q**, quadrate; **qj**, quadratojugal; **sa**, surangular; **so**, supraoccipital; **sof**, suborbital fenestra; **sp**, splenial; **sq**, squamosal; **sqg**, squamosal groove; **stf**, supratemporal fenestra.

SYSTEMATIC PALEONTOLOGY

CROCODYLIA Gmelin, 1789, sensu Benton and Clark, 1988
ALLIGATORIDAE Cuvier, 1807, sensu Norell et al., 1994
CAIMANINAE Brochu, 1999
BRACHYCHAMPSINI tax. nov.

RegNum Registration Number—1078.
Definition—The largest clade of alligatorids more closely related to *Brachychampsa montana* Gilmore 1911 than to *Caiman crocodilus* (Linnaeus 1758) or *Alligator mississippiensis* (Daudin 1802).
Reference Phylogeny— Figure 14 of this article.

Hypothesized Composition—Brachychampsini is currently hypothesized to include five named species: *Albertochampsa langstoni* Erickson 1972, *Brachychampsa montana* Gilmore 1911, *Brachychampsa sealyi* Williamson 1996, *Chrysochampsa mylnarskii* Estes 1988, and *Stangerochampsa mccabei* Wu et al. 1996.

Diagnosis—Brachychampsini is diagnosed on the character basis of a uniformly narrow scapulocoracoid facet anterior to the glenoid fossa, a large incisive foramen that intersects the premaxillary–maxillary suture, long dorsal premaxillary processes extending beyond the third maxillary alveolus, and a frontoparietal suture that makes modest entry into supratemporal fenestra at maturity and whose postorbital and parietal are in broad contact.

Etymology—The name Brachychampsini refers to the Greek words "brachy" for "short" and "champsa" for "crocodylian" as well as the Latin suffix "ini" to denote taxonomic tribe.

CHRYSOCHAMPSA MYLNARSKII Estes, 1988

Holotype—YPM VPPU.017258 (Figs. 3–5, 13), skull and mandible, intercentrum, osteoderms, one loose tooth, two dozen unidentifiable fragments.

Diagnosis—"A taxon distinguished from all other alligatoroid species except *Hispanochampsa muelleri* (Kälin, 1936, 1955) in the extremely narrow interorbital portion of the frontal and from all alligatoroid species by the great posterior width of the frontal with respect to the proportions of the skull as a whole" (Estes, 1988:553).

Emended Diagnosis—An alligatorid crocodylian diagnosed by a suite of shared and unique character states including: a keyhole shaped, dorsally projecting external nasal aperture that is flush with the dorsal surface of the premaxillae and contacted posteriorly for a very short distance by the blunt anterior nasals; dorsal premaxillary processes that are long, thin, and extend posteriorly to the fourth maxillary alveolus which is the largest in the maxillary toothrow; a frontal bone which is narrow in the interorbital region and extremely wide posteriorly such that the postorbitals do not form part of the orbital margins; a frontoparietal suture that makes modest entry into the supratemporal fenestra; a dentary symphysis that extends to the fourth dentary alveolus in dorsal view; a twelfth dentary alveolus which is the largest dentary alveolus distal to the fourth; a splenial whose anterior tip passes dorsal to the Meckelian groove and forms a slight contribution to the mandibular symphysis; an atlas intercentrum that is plate shaped in lateral view; dorsal osteoderms that are square in shape and do not bear keels.

Occurrence—Wasatchian age exposures of the uppermost Paleocene/Eocene Golden Valley Formation. Collected across from Turtle Valley below Coffin Butte, SW ¼ section 16, T138N, R98W. Stark County, North Dakota, U.S.A.

DESCRIPTION

Skull—Preservation of the skull, with the exception of the posteriormost upper and lower jaws, is three-dimensional (Figs. 3, 4). Deep cracks are present in some regions and have been repaired with a tan-colored adhesive depicted as hatched lines in the figures. Distortion is present along the length of the skull and mandible rendering some morphology impossible to interpret—these characters are unscored in the character/taxon matrix. Posteriorly, distortion is pronounced where compression and twisting in multiple planes is present—the infratemporal fenestrae, temporal bars, and otic region have been profoundly altered or destroyed. Upper and lower jaw joints are missing on both sides. The posterior skull elements are pushed anterodorsally rendering the exoccipitals, squamosals, and quadrates out of normal orientation (Fig. 4). In some regions of the skull,

dorsoventral compression has welded dorsal and ventral elements to one another. Ventrally, the lower jaw, many loose teeth, and chunks of bone adhere to the skull and obscure sutures and other relevant morphology for the phylogenetic analysis. Sculpturing of the dorsal elements is present but not prominent. Some dorsal elements appear abraded due to weathering, preparation, or other forces. The dorsal side of the specimen is darker in color than the ventral side likely due to weathering or other geological processes. In whole, the specimen is tan but many elements have a mottled appearance with small, darker brown splotches. This appearance is not to be confused with sculpturing as there are no corresponding impressions or raised areas in these regions. In dorsal view, the skull tapers in the frontal plane from posterior to anterior. The snout is broad, a third longer than wide, and is similar in outline to the Cretaceous alligatorids *Albertochampsa langstoni*, and species of *Brachychampsa* but distinct from the shorter snout of *Stangerochampsa mccabei*. The species is reconstructed as having an overbite due to the presence of occlusal marks medial to the maxillary toothrow. Due to the fragility of the specimen, lateral photographs and figures outside of the storage jacket are not feasible.

External Nasal Aperture—In the frontal plane the external nasal aperture opens dorsally (Fig. 3). Its margin is better preserved on the right side, some dislocation and ventral compression of the anterior left margin is present—the outline is key-hole shaped with the anteroposterior axis being longer than the mediolateral axis. The blunt anterior nasals contact the aperture and push into the structure for a very short distance—although size and shape of the aperture are similar to *S. mccabei* the anterior extent of the nasals within the aperture is shorter here. The premaxilla forms the anterior and lateral margins whereas the nasals form the posterior margin. The anterior margin is broadly concave, the lateral margin is reconstructed as nearly linear, and the posterior margin is convex due to the slight contribution of the nasals to the aperture. A modest uplift is present around the dorsal opening of the aperture but this uplifted region grades into the rest of the snout—no lips or indentations in the area surrounding the margin are present.

Incisive Foramen—Although obscured both dorsally and ventrally by adhering bone and dental material a large, teardrop-shaped outline of the incisive foramen is determined (Fig. 3). Ventrally, the margins of the structure are clearest on the right side. The lateral margins, formed by the premaxillae, extend laterally to the third premaxillary alveoli. The anteriormost point of the foramen, situated far from the toothrow and extending anteriorly to the point of the third alveolus, is directed toward the space between the first premaxillary alveoli on either side. Owing to its size and anteroposterior length, it is possible that the posterior aspect of the foramen intersects the premaxillary–maxillary suture, but this is not included in the phylogenetic analysis due to the obscure sutural contact. Character states in the phylogenetic matrix do not differentiate *C. mylnarskii* from other members of Brachychampsini but gross morphological comparison indicates similarities in incisive foramen size and shape between *C. mylnarskii*, *A. langstoni*, and *B. montana*.

Premaxilla—Both premaxillae are preserved but owing to the superior preservation of the right premaxilla, the proportions and morphology are better representations of the animal's morphology in life (Fig. 3). Dorsally, the element forms the anterior and lateral margins of the bony nasal aperture. The dorsal premaxillary processes are long, thin, and extend posteriorly to the fourth maxillary alveoli. Similar coding in the phylogenetic matrix belies the combination of shape and posterior extent of these features that differentiate *C. mylnarskii* from closely related brachychampsins. Ventrally, the premaxillary toothrow bears five alveoli on each side but no teeth. Although the
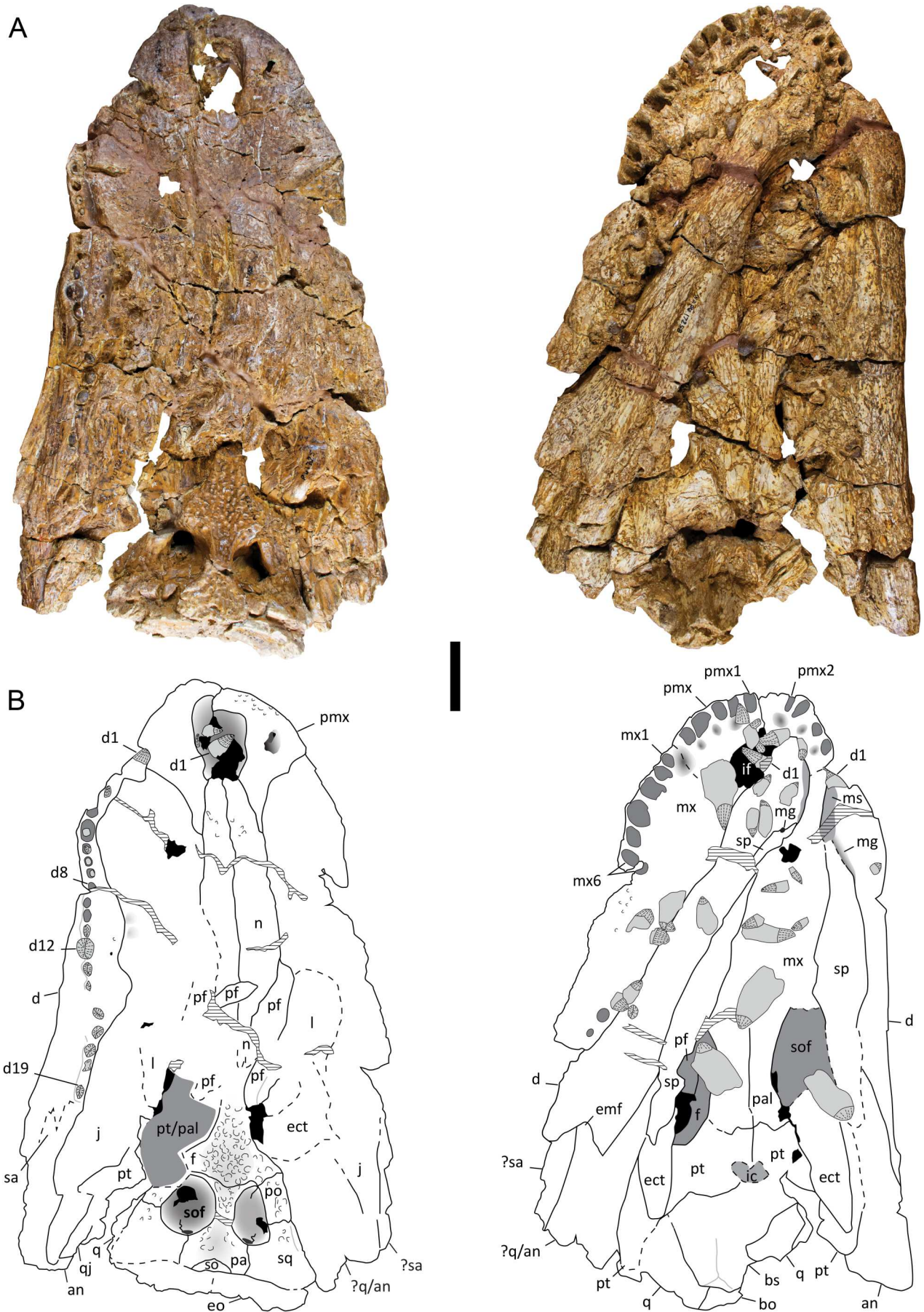
FIGURE 3. *Chrysochampsa mylnarskii*, YPM VPPU.017258 holotype specimen. **A**, pictures of skull in dorsal (left) and ventral (right) views. **B**, interpretive line drawings of skull in dorsal (left) and ventral (right) views. Scale bar equals 5 cm.
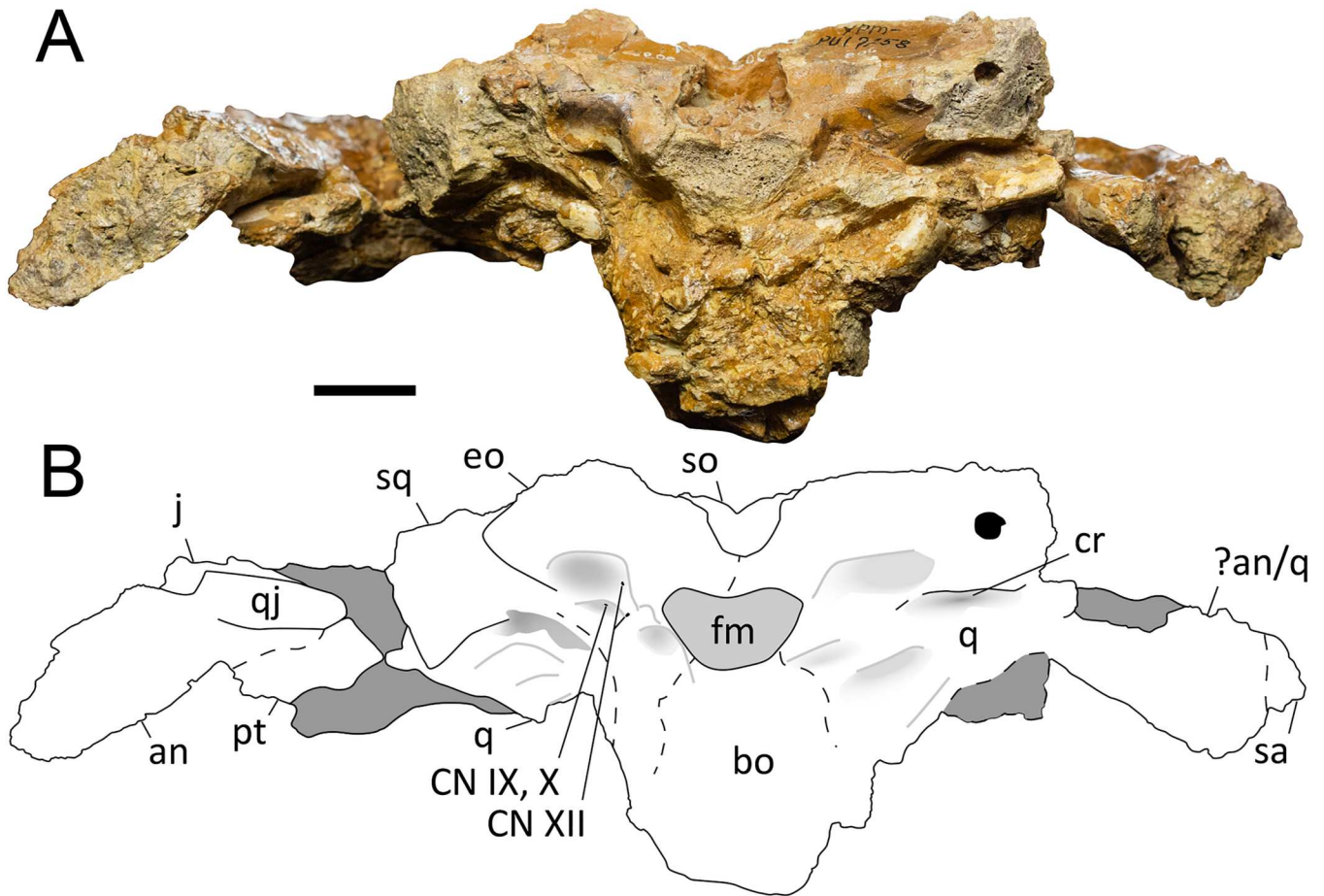
FIGURE 4. *Chrysochampsa mylnarskii*, YPM VPPU.017258 holotype specimen. **A**, picture of skull in occipital view. **B**, interpretive line drawing of skull in occipital view. Scale bar equals 5 cm.

margins of the alveoli are imperfect, the right premaxilla indicates that the first and second alveoli are relatively small in diameter, the third alveolus is larger, the fourth is largest, and the fifth is similar in size to the first and second. Although missing parts of their medial margins, the fourth and fifth alveoli of the right side appear to be larger than the left. Lingual to the toothrow, four indentations for the anterior dentary teeth suggest an overbite. Although shards of bone and dental material obscure the feature on the right side, a large indentation for the first dentary tooth lies lingual to the first and second premaxillary alveoli on the left premaxilla. Indentations for the second and third dentary teeth are lingual to premaxillary alveoli three and four, and four and five, respectively. Although not preserved on the left side, the right element bears a large indentation for the fourth dentary tooth at the premaxillary–maxillary suture. Occlusal marks appear to be deeper on the left relative to right —it is unknown whether this is due to diagenesis, pathology, or otherwise.

Maxilla—The maxillae experienced post-depositional alteration from compression and twisting in multiple planes (Fig. 3). Regardless, the dorsal surface of the element appears smooth with no bosses, ridges, or other protuberances. The left element experienced dorsoventral flattening anteriorly and mediolateral compression posteriorly. Gross comparison to brachychampsins indicates proportionally longer maxillae for *C. mylnarskii*. Anteriorly, the maxilla contacts the premaxilla in an extensive, concave, anterolaterally trending suture from posterior to

anterior. Medially, the maxillae and nasals meet at a linear, anteroposteriorly trending sutural contact that is proportionally longer than other brachychampsin species. On the left side nearly at mid-body, the maxilla is pushed laterally onto the left nasal. The posterior sutural contacts are harder to interpret but the maxillae likely made contact with the lacrimal and jugal. An area of contact with the prefrontal on the right side is clear and demonstrates a short, anteromedially trending suture from posterior to anterior. The maxilla sends a short, V-shaped projection posteriorly between the anterior prefrontal and lacrimal bones—most similar to *B. montana*. The right side of the maxilla experienced considerable dorsoventral crushing but likely preserves a better approximation of its lateral margin relative to the mediolaterally compressed left element. Between the first and sixth maxillary alveoli, the maxilla is laterally expanded in dorsal view. A second area of expansion is present posterior to this—the state of preservation hinders attribution to a region of alveoli. Characters describing the shape of the maxillary toothrow are unscored due to deformation and incomplete exposure but the right side is best preserved and the first six alveoli are identified to position. These alveoli increase in size from the first to the fourth position and then proceed to get progressively smaller. In common with *A. langstoni* and *S. mccabei*, the largest maxillary alveolus is in the fourth position. Distal to the sixth maxillary alveolus the identities of teeth and alveoli are difficult or impossible to determine—portions are missing or obfuscated by overlying bone. Distal to the sixth maxillary alveolus are

two socketed teeth presumed to represent either the seventh and eighth, or the eighth and ninth maxillary teeth. The mesialmost of these socketed teeth is small and conical and the distalmost tooth is large, low crowned, and has apicobasal striations. Distal to these teeth it is impossible to track alveolar position along the arcade and the last, low crowned, socketed tooth and two alveoli are separated from the mesial two socketed teeth by a distance of approximately 3 or 4 alveoli. On the ventral side, medial to the toothrow, deformation hinders exploration of the occlusal indentations produced by the overbite. Extensive alteration and overlying bone in the area of the suture with the palatines hinders interpretation.

Nasal—Preservation is good with the exception of the extensively cracked posteriormost portions (Fig. 3). Anteriorly, the nasals end in a blunt point forming the posterior margin of the external nasal aperture. Although other brachychampsins share a similar contact with the aperture, the very blunt anterior nasals and extremely short distance they traverse through the structure differentiate *C. mylnarskii* from those taxa. The nasals contact the premaxillae at an anteromedially oriented suture that trends gently toward the midline from posterior to anterior and ends at the posterolateral corner of the external nasal aperture. The mid-bodies of the elements contact the maxillae in long, nearly parallel sutural contacts. Posteriorly, the prefrontals contact the nasals—the suture is clear on the right side and trends anterolaterally from posterior to anterior. As interpreted here, the posteriormost nasals end in blunt points separated from one another by the anteriormost frontal at the midline. These points contact the frontal posteriorly and the prefrontal posterolaterally.

Orbit—Although incompletely preserved on both sides, the dorsal elements contributing to the margins of the orbit are determined with certainty. The anteromedial margin is formed by the prefrontals, medial and posterior margins are formed by the frontals (Fig. 3)—the postorbitals do not appear to form a margin of the orbit and differentiates *C. mylnarskii* from phylogenetically allied species. Depending on interpretation of contributing elements and restoration of deformation, the lacrimal formed the anterolateral margin and the jugal formed the lateral margin. A slight ridge along the medial margin of the orbit is formed by contributions of the prefrontal and frontal. Preservation hinders identification of a ridge along other margins of the orbit.

Prefrontal—The prefontals are distorted and broken but the right side is better preserved (Fig. 3)—a large break is present nearly half-way along its anteroposterior length but gives a good indication of the anterior and posterior morphology of the element and its sutural contacts. Medially, the prefrontal makes contact with the nasal along a long sutural contact, trending mediolaterally from posterior to anterior. The anteriormost element forms a short sutural contact with the maxilla that is oriented mediolaterally from anterior to posterior. Laterally, the prefrontal contacts the lacrimal at a long, anteroposteriorly linear, suture. The posteriormost prefrontals appear to be separated from the nasals by a roughly anteroposterior sutural contact with the frontal. The right element preserves part of the anteromedial margin of the orbit and a ridge along the dorsal side of the element contributes to the slight ridge along the medial aspect of the orbit.

Lacrimal—Extensive damage to the right lacrimal results in tentative identification of margins. A roughly ovoid chunk of bone presumed to represent the left lacrimal indicates that the element forms the anterolateral orbital margin (Fig. 3). A long posterior process of the element forms an extensive, anteroposteriorly oriented sutural contact with the jugal on the left side. The anterior extent of the left element cannot be determined due to extensive cracking but tentative identification of the right jugal allows for tracing of its anterior margin—the

anteriormost extent of the element is broad and ends in a blunt point closely resembling *B. montana* and *S. mccabei*.

Jugal—The right jugal is preserved but its margins are impossible to define save a section of its mid-body (Fig. 3). Margins are clear along much of the left jugal's length—its posteriormost tip ends in a point shifted relative to the main body of the element. The element is nearly as wide anteriorly as at mid-body and tapers to a point posteriorly. The jugal bears an expansion in the region of the reconstructed lateral margin of the left orbit—this region is mediolaterally oriented due to crushing but dorsoventrally aligned in life. The postorbital bar is not preserved. The lateral aspect of the element forms the posterolateral margin of the skull, is altered but appears to have been linear in outline.

Quadratojugal—The margins of the right element are obscure but the posteriormost extent of the left element is preserved (Fig. 3). Laterally, the quadratojugal contacts the posteriormost jugal at a linear sutural contact with the angular, and the preserved posterior tip of the element extends almost to the same point as the jugal. Medially, the element makes contact with the quadrate. Preserved portions indicate an element whose outline differs in posterior width relative to phylogenetically allied species.

Quadrate—Dorsally, the margins of the quadrates are difficult to discern and their contribution to the upper jaw joint are missing (Fig. 3). A small fragment of the left element is preserved. It forms the medial aspect of the element along the ventrolateral skull table (Fig. 4), but is compressed against the squamosal hindering a more complete description. The margins of the right element are largely unidentifiable and like its left-side counterpart is compressed, cracked, and moved dorsally out of its normal orientation. Posteriorly, the contribution of the quadrates to the occipital region of the skull are incompletely preserved (Fig. 4). The quadrate forms the ventral and lateral margins of the external surface of the cranioquadrate canal which is best preserved on the right side. Along the lateral margins of the occiput, the quadrate sends short ventral processes along the exoccipitals. Evidence for these ventral processes is clearer on the left side, and the suture with the exoccipital is very slight whereas it is not visible on the right. On the left side a fragment of bone tentatively identified as a part of the quadrate, is adhered to the ventral side of the posterior skull. Ventrally, the right element is best preserved but whose margins are difficult to discern in part due to obfuscation by the posterior pterygoid process. A sutural contact between the incompletely preserved basisphenoid and quadrate is clear and trends mediolaterally from anterior to posterior. Due to extensive alteration in relevant areas, character coding of the element is incomplete.

Skull Table—All skull table elements are preserved and the structure is roughly triangular with the posterior margin about twice as wide as the anterior (Fig. 3) and much wider than seen in closely related taxa. Considerable distortion shifted posterior elements anteriorly and right-side elements medially. When viewed from a posterior perspective the parietal and supraoccipital trend ventrally from lateral to medial (Fig. 4), but alteration of the skull table hinders diagnosing it as entirely planar. Two expansive, dorsal midline indentations are deepest at their respective midpoints. Between the orbits and supratemporal fenestrae, the frontal and anteriormost parietal bear a longer than wide rhomboidal indentation. The second indentation is also rhomboidal, nearly as wide as it is long, and lies on the posterior parietal and dorsal supraoccipital. The dorsal skull table preserves the most pronounced sculpturing among skull elements. Collectively, the proportions of constituent skull table elements and structures in *C. mylnarskii* differ from other brachychampsins.

Supratemporal Fenestra and Fossa—The supratemporal fenestrae are preserved—the right side is complete, but compression

of the lateral skull table renders the lateral margin of the fenestra out of its original orientation (Fig. 3). The left side is missing a small portion of the anterolateral margin formed by the postorbital, but is likely a better approximation of shape in life. Reconstruction of the supratemporal fenestrae indicates that the structure is large and semicircular with a posterior margin that is more expansive than the anterior, a linear lateral margin that trends mediolaterally from anterior to posterior, and a broadly concave medial margin. The parietal and postorbital form the anterior margin, the postorbital and squamosal comprise the lateral, the squamosal and parietal contribute to the posterior, and the parietal forms the medial margin in its entirety. The margins of the supratemporal fenestrae gradually transition to the supratemporal fossae—no rim or overhang is present. A three-way sutural contact between the frontal, postorbital, and parietal makes an extremely modest entry into the right supratemporal fenestra, and the sutural contact between the parietal and postorbital continues ventrally along the anterior wall of the supratemporal fossa. Brachychampsins preserve frontoparietal sutures that make modest entry into the supratemporal fenestrae. Along the posterior wall of the supratemporal fossa, the parietal and squamosal form a suture also found in its closest relatives, but absent from *B. montana*. This contact intersects the temporoorbital foramen along the midpoint of its dorsal margin and at the ventrolateral margin of the foramen continues for a short distance into the depths of the fossa. Within the fossa, the sutures are clear along the dorsal half of the structure but become difficult or impossible to follow ventrally.

Temporoorbital Foramen—An oval foramen for conveying the temporoorbital vessels lies along the posterior wall of the supratemporal fossae (Fig. 3). The parietal forms the ventral, medial, and medial half of the dorsal margin. The squamosal forms the lateral margin and lateral half of the dorsal margin.

Frontal—Dorsally, the element is roughly triangular with the base of the shape facing posteriorly (Fig. 3). Margins of the anterior frontal are obscured by deformation and cracking—no characters were scored for this region. The element is complete with the exception of the posterolateralmost left side. Posteriorly, the element is mediolaterally expansive, and forms the entire posterolateral margin of the orbit—a diagnostic feature unknown for other crocodylians. As the frontal trends anteriorly, forming the medial margins of the orbits, it is progressively constricted. The frontoparietal suture is posteriorly convex and shared with all brachychampsins. As indicated on the right side all but its lateralmost corner lies anterior to the supratemporal fenestra and does not meaningfully contribute to it. The right-side sutural contact between the frontal and postorbital is nearly linear and trends anterolaterally from posterior to anterior.

Postorbital—The right element is complete but the anterior left postorbital is not preserved. The element forms the anterolateral margin of the skull table, and part of the lateral margin of the supratemporal fenestra (Fig. 3). The rectangular shape of the element and lack of contribution to the orbit differentiates *C. mylnarskii* from all close relatives whose postorbitals are boomerang shaped and form the posterior orbital margin. Anteriorly, the postorbital meets the frontal in a nearly linear suture that trends anterolaterally from posterior to anterior. Along the anterior wall of the supratemporal fossa, the element meets the parietal at a ventrally trending sutural contact. Compressive forces obscure the right element and ventral elements pushed into its lateral surface render coding of the postorbital bar impossible. Both sides demonstrate that the element contributes to the anterior extent of the squamosal groove. Posteriorly, the postorbital meets the squamosal at a nearly linear sutural contact that gradually trends anterolaterally from posterior to anterior.

Parietal—Although entirely preserved, a crack is present at mid-body. Dorsally, the element is hourglass shaped and distinctly wasp-waisted between the supratemporal fenestrae

(Fig. 3). A depression along the midpoint of its dorsal surface is deepest posteriorly and is confluent with the supraoccipital. Anteriorly, the element contacts the frontal and postorbital, and posteriorly contacts the broadly exposed supraoccipital at an anteriorly convex suture reaching the posterior margin of the skull table via large processes lateral to it. The parietal forms the medial margin of the supratemporal fenestra and the medial wall of the supratemporal fossa. The parietal forms the entirety of the ventral, medial, and lateral half of the dorsal margin of the temporoorbital foramen. Posterolaterally, the element contacts the squamosal at an anteroposteriorly trending and laterally convex suture.

Squamosal—The squamosal is boomerang shaped in dorsal view with the point of the angle facing posterolaterally (Fig. 3). The squamosal groove is most clearly preserved on the right squamosal and postorbital and indicates that the dorsal and ventral rims for the external ear valve musculature are parallel. Although the posterior skull experienced deformation, the body of the squamosal is intact and indicates that the element is planar in lateral perspective bearing no dorsal protuberances. The posterolateral rami of the squamosals are deformed and posteriorly chipped away—it is impossible to indicate whether the skull table has short or significant posterolateral rami along the paroccipital processes (Fig. 4).

Supraoccipital—Common to *C. mylnarskii* and species of *Brachychampsa*, but differentiating them from *S. mccabei* and *A. langstoni* the supraoccipital is large and broadly exposed on the dorsal skull table (Fig. 3). It is more than three times as wide as it is long, and shaped like a crescent moon with the convexity of the shape pointing anteriorly at the sutural contact with the parietal. The midline of the element, exposed on the dorsal skull table, preserves a depression confluent with the parietal. From a posterior perspective, the element is approximately triangular with the widest point dorsally and a blunt point facing ventrally (Fig. 4). The element meets the exoccipital at a short mediolaterally trending suture from ventral to dorsal. Due to alteration, the posttemporal fenestrae are obscure and the posterior element is pushed anteriorly—yet the exposure is proportionally smaller than its closest relatives.

Foramen Magnum—The foramen is infilled with matrix but the margins are clear (Fig. 4). It is heart-symbol shaped with a gently rounded ventral tip. The exoccipitals form the dorsal and lateral margins of the structure and the basioccipital forms the ventral margin.

Exoccipital—The exoccipitals are deformed but preserved on both sides. The dorsalmost margins are pushed anteriorly and the medialmost margins are crushed between their contribution to the dorsal margin of the foramen magnum and the sutural contact with the supraoccipital (Fig. 4). The lateral margins of the foramen magnum, formed by the exoccipitals, are clear. The lateralmost paroccipital processes are missing and the right side preserves an unknown foramen that is confluent with an undetermined canal (Fig. 4). This structure, independent of the cranioquadrate canal found at the juncture of the exoccipital and quadrate, may represent the air sinus system. Three foramina are present on the left side lateral to the foramen magnum but obscured on the right. The lateral opening represents the jugular foramen and is for the conveyance of cranial nerve (CN) IX, X, and the jugular vein whereas the medial two foramina are for CN XII. The foramen for the carotid artery cannot be identified ventral to these structures. Ventrally, descending processes of the exoccipital are interpreted as lying lateral to the basioccipital. Evidence for the exoccipital–basioccipital suture is slight but interpreted as broad and laterally convex in shape.

Basioccipital—The posterior face of the basioccipital experienced considerable alteration and much of its morphology is indiscernible. Obliteration of the occipital condyle does not

hinder identification of the element's contribution to the ventral margin of the foramen magnum (Fig. 4). Inferior to this point the element expands mediolaterally and makes contact with the ventral processes of the exoccipital. The basioccipital makes broad contact with the basisphenoid ventrally (Fig. 3) but poor preservation warrants no further explanation here.

Basisphenoid—The basisphenoid is cracked and twisted. Exposure of the anteroventral face demonstrates a keel shifted into a parasagittal orientation right of the midsagittal plane (Fig. 3). In life, the medial aspects of the pterygoids would cover this keel.

Suborbital Fenestra—Both sides preserve portions of the suborbital fenestrae (Fig. 3). Complete margins are impossible to determine—the mandible covers the anterior margin on the right side and obscure sutural contacts make interpretation difficult on the left side. Medial margins are clear and are formed by the palatines, which are gently bowed with the convexity of the fenestra facing medially. The pterygoid forms the bowed posterior margin, as preserved on the right side, and the ectopterygoid forms the posterolateral margin as seen on the left side. Although incompletely preserved, the suborbital fenestrae of *C. mylnarskii* appear relatively larger with an anteroposteriorly oriented midline in opposition to the smaller, obliquely trending fenestrae of *B. montana*, *S. mccabei*, and *A. langstoni*.

Palatine—Morphology is obscured along points on both sides, yet, enough of the elements and their sutural contacts are exposed to provide a holistic appraisal of their morphology. A break transects the anterior right element and is infilled with a brown adhesive (Fig. 3). Adherence of a tooth and the overlain hemimandible conceals parts of the right element. Anteriorly, the sutural contacts with the maxilla are obscured by a tooth and cracking—the state of the anterior process is unknown. A linear, midsagittal suture connects the right and left elements. The lateral edges of the palatines are smooth anteriorly and taper mediolaterally into a waist at the elements' mid-body forming the broadly curving medial margins of the suborbital fenestrae. Within this region, the posterolateral edges of the palatines flare to produce a small shelf over the depths of the posterior suborbital fenestrae. Anterior to the sutural contact with the pterygoids, a break is present—although this complex, mediolaterally trending suture is well preserved, it is impossible to determine where it contacted the posterior margin of the suborbital fenestra and prevents character coding. In gross appearance, the palatines are relatively longer and less robust compared with phylogenetically allied brachychampsins.

Ectopterygoid—The ectopterygoids are broken and distorted. Preservation of the left element is best. The body of the right element is pushed dorsally rendering it visible lateral to the frontal bone on the dorsal side of the skull—from this view the maxillary and jugal processes are visible, with the former being anteroposteriorly more extensive than the latter (Fig. 3). Ventrally, the ectopterygoid–pterygoid flexure that disappears during crocodylian ontogeny is absent in this mature specimen. As preserved on the left side, the ectopterygoid forms the posterolateral margin of the suborbital fenestra. However, due to poor preservation the character describing the shape of the margin is unscored in the phylogenetic matrix. Although the ectopterygoid contributes to the lateral margin of the suborbital fenestra, the proportion that it forms cannot be determined due to poor preservation on the left side and the overlying right hemimandible on the right side. Additionally, preservation does not allow for an assessment of the abutment of, or absence of, the ectopterygoid along the maxillary toothrow. The pterygoid processes on both sides are preserved. The more complete right side indicates that the process ends in a blunt tip short of the posterior end of the lateral pterygoid flange.

Pterygoid—Pterygoids are mediolaterally broad and anteroposteriorly expansive (Fig. 3). Relative to species of brachychampsins, the elements are similarly wide as *B. montana* but exceed all species in length. Alteration renders the elements visible on both the dorsal and ventral sides of the skull. They experienced considerable cracking, their posterior and lateral margins are difficult to follow, and are bonded to various elements. Dorsally, parts of the left pterygoid are adhered to the left palatine and visualized through the area of the orbit and infratemporal fenestra. Additional remnants of the pterygoid, compressed against the jugal and quadratojugal, are along the dorsal left side of the skull (Figs. 3, 4). Ventrally, the elements meet the palatines along a complex mediolaterally trending suture and meet one another along an anteroposteriorly linear midline suture. Although the pterygoids form all preserved margins of the internal choanae, at the posterior midline the contribution of the pterygoids to the posterior margin of the structure is missing. Laterally, the pterygoid wings become progressively more expansive. These features end in an expanded lateral pterygoid buttress whose ventrolateral surface parallels the ectopterygoids for a distance.

Internal Choanae—Some distortion is present in the area around the choanae but preserved margins indicate a heart-symbol shaped structure (Fig. 3) most similar in morphology to *S. mccabei*. The anterior margin is composed entirely of the pterygoids, with the margin flush with their surface. Parts of the lateral margin and the entire posterior margin are missing—based on comparison to known eusuchians the remaining margins must also have been composed of the pterygoids. The missing margins hinder the description of the directionality of the choanae's opening and the inclusion of the resulting character state in the phylogenetic analysis. The pterygoid is flush with the remaining margins and the anterior part of the septum is recessed inside the structure.

Mandible—The anterior and mid-jaw elements are nicely preserved but altered by a few, large cracks and repaired using a tan-colored adhesive—these are depicted as hatched lines in the dorsal and ventral figures of the specimen (Fig. 3). The posterior-most jaw, including the jaw joints, is missing. Preserved portions of the disassociated hemimandibles suggest a robust, broadly curving mandible. The left side of the mandibular symphysis is best preserved and crushing of the right side makes it appear longer than the left. Although mostly formed by the dentary, the splenials provide a slight contribution to the mandibular symphysis. Here the dentary symphysis extends to the fourth dentary alveolus (Fig. 13F) and differentiates it from close relatives whose dentary symphyses extend considerably beyond this point. A break midway through the eighth dentary alveolus renders the anterior jaw slightly out of line with the posterior jaw—it is impossible to code characters describing the shape of the toothrow although many alveoli are in their natural position.

Dentary—Both dentaries are preserved yet separated at the mandibular symphysis and out of normal orientation (Fig. 3). Rugose lineations interspersed with pits cover the lateral surfaces of the elements. Interpretation suggests that the lineations are products of postmortem cracking and the pits represent neurovascular foramina and sculpturing. Both right and left elements are adhered to the ventral side of the skull obscuring the dorsal surface and toothrow on the right side, but pushing the left element laterally to expose the toothrow from a dorsal perspective. The right dentary preserves the anterior margin of the external mandibular fenestra—incomplete preservation renders the structure unscorable in the phylogenetic analysis. The left hemiarcade indicates 19 alveoli per hemimandible and most of the toothrow is in its natural position. All alveoli and teeth are circular to ovoid in cross section with teeth bearing a slight carina, apicobasal striations of the enamel, and moderate buccolingual compression along the posterior toothrow. Among the anterodorsally projecting anterior dentary teeth the first tooth is large and conical, and oriented anteriorly as a result of distortion.

The second and third alveoli get progressively larger, and the fourth is the largest in the mandibular arcade. Although not preserved in contact, in life the large fourth dentary tooth would have occluded into the pit at the juncture between the ventral premaxilla and maxilla. Relatively large diastemata are present between the first and second, and second and third alveoli. The alveoli for dentary teeth three and four are separate and relatively close to one another. Alveoli in positions five through 11 get progressively smaller, and then larger and bear subequal spaces between them. The twelfth alveolus bears the second largest tooth in the lower jaw and the largest tooth posterior to position four, the thirteenth alveolus bears a relatively large tooth, and the following six alveoli are in various states of preservation, nearly equal in size and bear teeth with low crowns and slight buccolingual constrictions. Large diastemata are present between alveolar positions 14 and 15, and 18 and 19. These features do not appear to be the result of distortion. Teeth preserved in alveolar positions 1–2 and 11–19 are relatively complete or complete, whereas teeth in positions 4–7 are missing their crown or have yet to erupt from the depths of the alveolus. In lateral view, the toothrow is uplifted in the region of the fourth dentary alveolus and between alveolar positions 11–13 with the apex of the uplift at the twelfth alveolar position (Fig. 13F) (incorrectly reported as at point of tooth 13 in Lucas and Sullivan [2004]).

Splenial—Splenials are preserved and best viewed on the ventral side of the skull (Fig. 3). Large cracks cross both elements—a brown adhesive fills some of them. In its current orientation, the wedge-shaped medial surface of the element is oriented ventrally. The anterior margins of the right splenial preserves an anterior process dorsal to the Meckelian groove similar to species of *Alligator* and some caimanines, but differentiating *C. mylnarskii* from its closest relatives. The foramen for CN V_3 exits at the anterior Meckelian groove inferior to the dorsal projection of the symphyseal process of the splenial in common with *B. montana* but differentiating it from *S. mccabei*. Dark brown spots on a tan background mottle the medial aspect of the splenial and, if preserved, obscure the presence of small foramina. The splenials do not preserve evidence for foramina intermandibularis.

Other Lower Jaw Elements—Ventrally, portions of the right surangular and angular are tentatively identified (Fig. 3). These share a long anteroposteriorly trending sutural contact, but do not preserve morphology relevant to the phylogenetic analysis. The left hemimandible preserves sutural contacts whose position and shape indicates that they may be the posteriormost contact between the splenial and angular. The left angular contacts the dentary at a long, dorsoventrally trending suture. Dorsally, the left surangular is difficult to identify but from the preserved portions, the anterior processes of the surangular are subequal as is common to alligatoroids—this feature is figured but not scored.

Atlas Intercentrum—A partial atlas intercentrum is preserved, the posteriormost extent is missing including the parapophyseal processes (Fig. 5A). It is dorsoventrally flat, or plate shaped, in lateral view as is common to alligatorids in this analysis.

Osteoderms—Four osteoderms are preserved (Fig. 5B) but only one is sufficiently preserved to comment on shape—in dorsal view it is nearly square, similar to most alligatorids and differentiating it from species of *Brachychampsa*. Three do not have a keel and the fourth, which is extensively cracked, preserves modest dorsal bowing along its ventral midline. The ambiguous evidence of a keel-like structure preserved via bowing on a single osteoderm does not overcome the preponderance of evidence preserved in the other three. Here, similar to all other alligatoroids in this analysis with the exception of *S. mccabei*, osteoderms are scored as unkeeled in the phylogenetic analysis.

Unidentifiable Element—A fragment of bone is associated with the holotype material at YPM (Fig. 5C). This fragment is not mentioned in Estes (1988) or Lucas and Sullivan (2004).
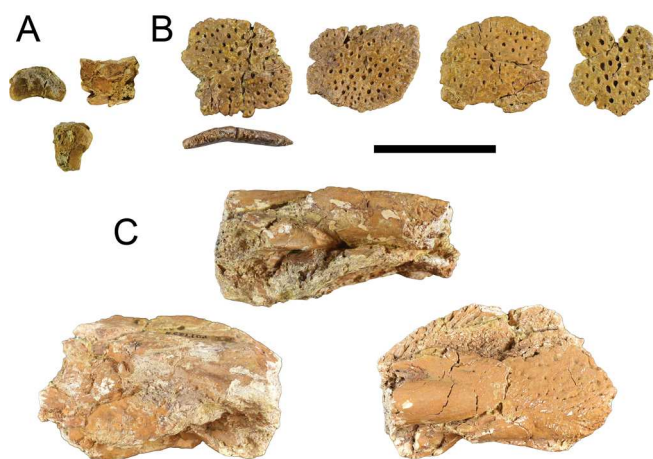

FIGURE 5. *Chrysochampsa mylnarskii*, YPM VPPU.017258 holotype specimen. **A**, atlas intercentrum in anterior view (upper left), dorsal view (upper right), and lateral view (bottom). **B**, osteoderms in dorsal view (top) and anterior view (bottom). **C**, fragment in various views. Scale bar equals 5 cm.

Coloration, texture, and three-dimensionality differs from the skull and associated postcranial elements. This complex fragment composed of various elements sutured to one another may represent a fragment of posterior lower jaw, including the articular.

Miscellaneous and Missing Elements—Approximately two dozen small, unidentifiable fragments are associated with the specimen. Two small teeth are associated with the type, one of which has a tall crown and appears to be the right size for this specimen. The other, which is darker than the other elements, is small, tall crowned, and likely did not belong to this specimen. Field notes of Jepsen (APC personal communication with D. Brinkman, YPM, 2023) do not reveal the nature of their recovery.

Estes (1988) introduces isolated vertebrae as forming part of the holotype. These elements, neither figured nor described, are not included in the holotype material by Lucas and Sullivan (2004). Examination of the holotype at YPM by one of the authors (APC) revealed that no vertebrae, other than the atlas intercentrum, are associated with the type specimen.

ALLIGATORINAE Gray, 1844
AHDESKATANKA RUSSLANDDEUTSCHE gen. et sp. nov.
(Figs. 6, 7, 8, 9, 10, and 13)

Holotype—YPM VPPU.016990 (Figs. 6–10, 13), skull, isolated mandibular elements, 10 loose teeth.

Referred Specimens—YPM VPPU.030620, left premaxilla. YPM VPPU.030623, left surangular. YPM VPPU.016902 (large) left dentary. YPM VPPU.016902 (medium) right dentary. YPM VPPU.016902 (small) right dentary. YPM VPPU.030621, left dentary. YPM VPPU.016996 right and left dentaries.

Diagnosis—An alligatorine crocodylian diagnosed by a suite of shared and unique character states including: large, symmetrical external nasal aperture that is nearly as long as it is broad and whose lateral margin is linear; dorsal premaxillary processes that are long, posteriorly thin, and extend to the sixth maxillary alveolus; large incisive foramen that intersects the premaxillary–maxillary suture and whose posterior margin is formed by the maxilla; a short sutural contact between the
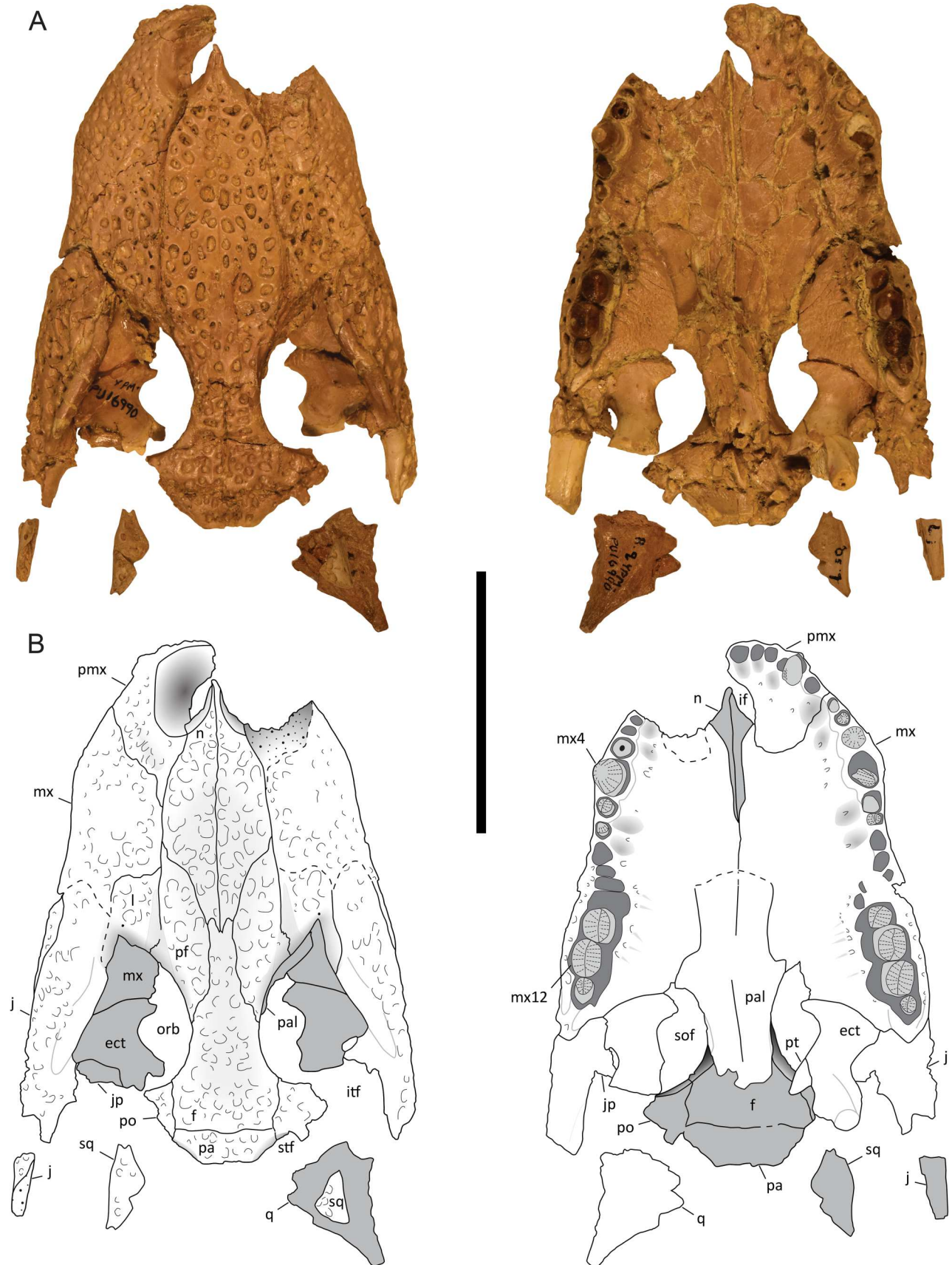
FIGURE 6. *Ahdeskatanka russlanddeutsche*, YPM VPPU.016990 holotype specimen. **A**, pictures of skull in dorsal (left) and ventral (right) views. **B**, interpretive line drawings of skull in dorsal (left) and ventral (right) views. Scale bar equals 5 cm.
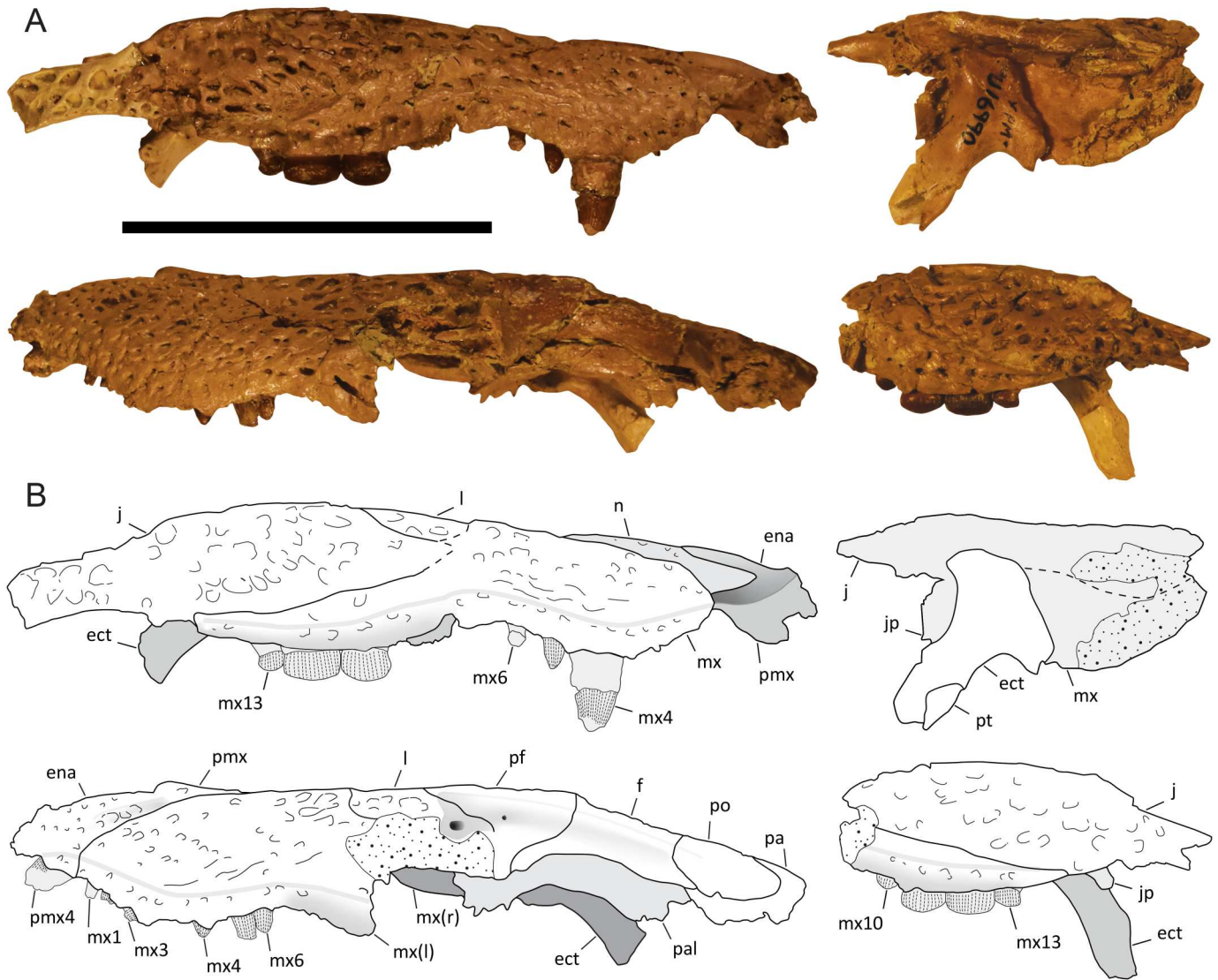
FIGURE 7. *Ahdeskatanka russlanddeutsche*, YPM VPPU.016990 holotype specimen. **A**, pictures of skull (counter-clockwise from top left), right lateral view, left lateral view, left posterolateral fragment in lateral view, left posterolateral fragment in medial view. **B**, interpretive line drawings of skull (counter-clockwise from top left), right lateral view, left lateral view, left posterolateral fragment in lateral view, left posterolateral fragment in medial view. Scale bar equals 5 cm.

maxilla and nasal; a prefrontal whose anterior extent greatly exceeds the lacrimal; anterior extent of jugal is subequal to the anterior lacrimal with a process of the maxilla between them; a linear frontoparietal suture; large, globular distal maxillary teeth whose penultimate tooth is more than twice the diameter of the ultimate.

Etymology—*Ahdeskatanka* (pronounced ah-de-shka-tan-ka), from Dakota Ahdeškataŋka, 'alligator'; in reference to the species occurrence in lands currently and historically inhabited by Dakota language speaking peoples; *russlanddeutsche*, from German russlanddeutsche, 'Germans from Russia', to acknowledge ethnic Germans who left the Russian Empire during the last decades of the 19th century and today call central and western North Dakota home.

Occurrence—Wasatchian age exposures of the uppermost Paleocene/Eocene Golden Valley Formation just above the hard siliceous layer. Turtle Valley Site, SW ¼ section 16, T138N, R98W. Stark County, North Dakota, U.S.A.

DESCRIPTION

Skull—The specimen consists of a three-dimensionally preserved skull but some posterior cranial elements are missing (Fig. 6). Although the entire skull experienced moderate dorsoventral compression during burial, as preserved the skull is dorsoventrally deep, especially so posteriorly (Fig. 7). Cracking is more pronounced on the ventral surface relative to dorsal and distortion renders some morphology impossible to interpret for the phylogenetic analysis. Associated with this specimen are 20 loose, unidentifiable cranial fragments, 19 of which likely represent the posteroventral portions of the skull or lower jaw (Fig. 8). Sculpturing on the dorsal surface of the skull is predominated by large, round to sub-round impressions. Most are individual, less are confluent and laterally the degree of ornamentation decreases with the lateral maxilla and premaxilla having the least pronounced ornamentation and a stippled appearance. In dorsal view, the skull tapers in the frontal plane from posterior to
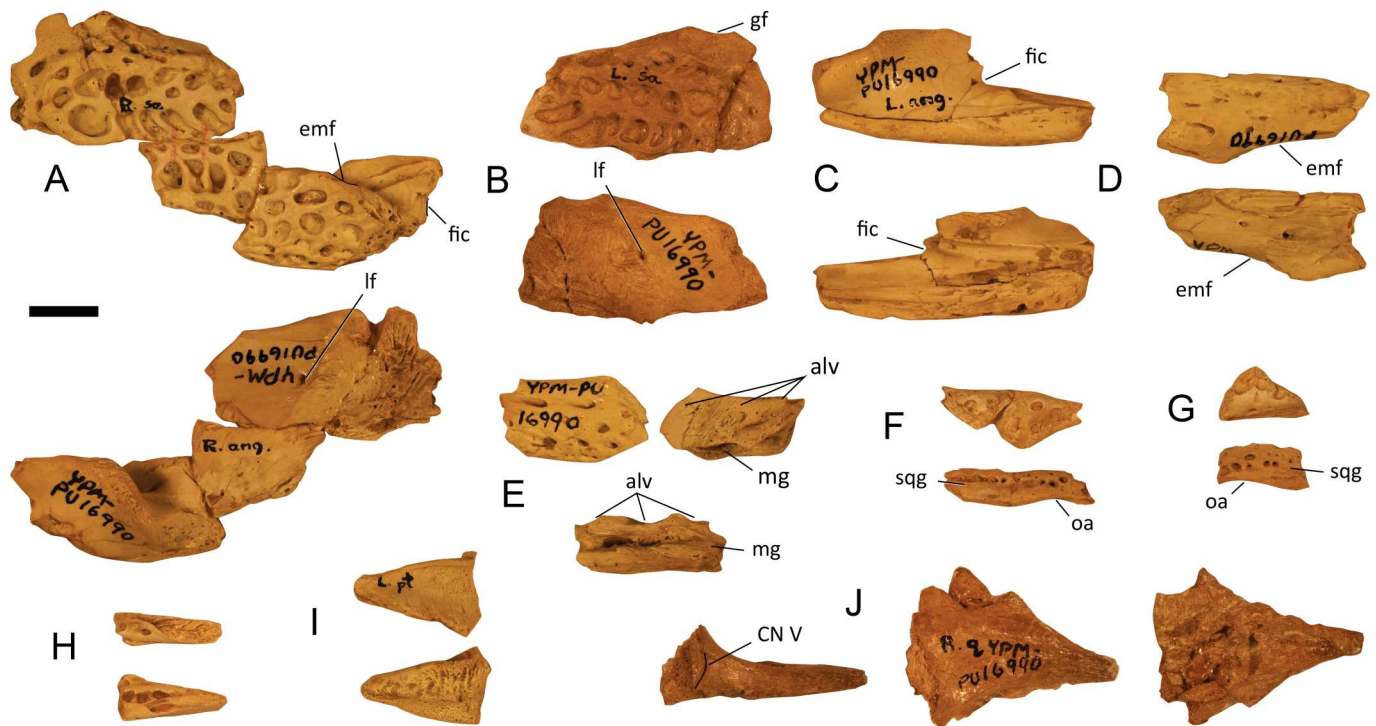
FIGURE 8. *Ahdeskatanka russlanddeutsche*, YPM VPPU.016990 holotype specimen. **A**, right surangular and angular in lateral (top) and medial (bottom) views. **B**, left surangular in lateral (top) and medial (bottom) views. **C**, left angular in medial (top) and lateral (bottom) views. **D**, right surangular in lateral (top) and medial (bottom) views. **E**, dentary in lateral (top left), medial (top right), and ventral (bottom) views. **F**, left squamosal in dorsal (top) and lateral views (bottom). **G**, right squamosal in dorsal (top) and lateral (bottom) views. **H**, left jugal in dorsal (top) and lateral (bottom) views. **I**, left pterygoid in dorsal (top) and ventral (bottom) views. **J**, right quadrate in anteroventral (left), ventral (middle), and dorsal (right) views. Scale bar equals 1 cm.

anterior, bears a slight ventral indentation of the midline elements and is exclusive of bosses, ridges, or canthi rostralii. The snout is very broad—nearly as long as it is wide—common among many small bodied, blunt tooth bearing alligatorids of this interval (Brochu, 2004). Occlusal marks medial to the maxillary toothrow indicate the presence of an overbite with all dentary teeth occluding lingual to the premaxillary and maxillary toothrow.

External Nasal Aperture—In the frontal plane the aperture projects anterodorsally with margins that are roughly flush with the surface of the premaxilla (Figs. 6, 7). Dorsally, the aperture is approximately circular in shape but larger and more equally proportioned in outline relative to closely related species in this analysis (Fig. 9). The premaxilla contributes to the anterior, lateral, and posterior margins of the aperture. The nasals broadly enter the aperture, travelling along half of its anteroposterior length, but do not bisect it and form the remaining margins of the aperture as is similar for all close relatives preserving the region. Each hemisphere of the aperture preserves a broadly concave anterior margin, linear lateral margin, and tightly concave posterior margin. No close relatives preserve similarly shaped and proportioned apertures, and only *Procaimanoidea utahensis* has a linear lateral margin but is consistently differentiated from the whole aperture morphology of *A. russlanddeutsche* (Fig. 9).

Incisive Foramen—The margins of the structure are complete on the left side and indicate a teardrop shape with the point of the form facing anteriorly (Fig. 6). Anteriorly and laterally, the margin is composed of the premaxilla. The maxillae form the posterior margin—taphonomic distortion separates the elements at the midline. The foramen is large, yet separated from the toothrow and extends anteroposteriorly from the level of the

fourth premaxillary alveolus to the third maxillary alveolus and intersects the premaxillary–maxillary suture. The combination of the foramen's large size and intersection of the premaxillary–maxillary suture is unlike all close relatives, but similar to species of *Brachychampsa* and *S. mccabei*.

Premaxilla—The left element is complete, but only the palatal lamina of the right element is preserved (Fig. 6). The right premaxilla dislocated from the skull at its contact with the nasal and maxilla, which respectively preserve the corresponding sutures—these agree with their left-side counterparts. Dorsally, the element forms a majority of the external nasal aperture's margins. Although the maxilla forms the lateral walls of the narial canal, dorsoventral compression obscures the internal morphology relevant to the phylogenetic analysis. Posteriorly, the dorsal premaxillary processes are long and extend to the posterior margin of the sixth maxillary alveolus. These processes are longer and posteriorly more slender than all close relatives in the analysis. A very modest indentation of the dorsal premaxillary surface parallels the premaxillary–maxillary suture and posterolateral margin of the external nasal aperture—but not to the degree as seen in similarly sized *Alligator mississippiensis*, for example, and is scored as a smooth premaxillary surface in the phylogenetic analysis. The depth of this feature is similar to *A. polyodon* whose indentation lies along the premaxillary–maxillary suture and is not applicable to this character. Ventrally, the element sends a broad palatal lamina posteriorly, similar to the interpretation of *Navajosuchus mooki*. These structures, separated medially by the incisive foramen and the maxilla, do not contact their counterpart. The suture for this process is clear on the left side but crushing obscures on the right. The dental hemiarch of the premaxilla preserves five alveoli. The fourth alveolus is large and bears a lingually displaced tooth that

FIGURE 10. Reconstruction of *Ahdeskatanka russlanddeutsche* right mandible based on YPM VPPU.016990 holotype specimen and YPM VPPU.016902 (medium dentary). Line drawing indicates mirrored elements including YPM VPPU.016990 left angular and YPM VPPU.016902 dentary. **A**, pictures of elements forming reconstructed right mandible. **B**, interpretive line drawing of elements forming reconstructed right mandible.
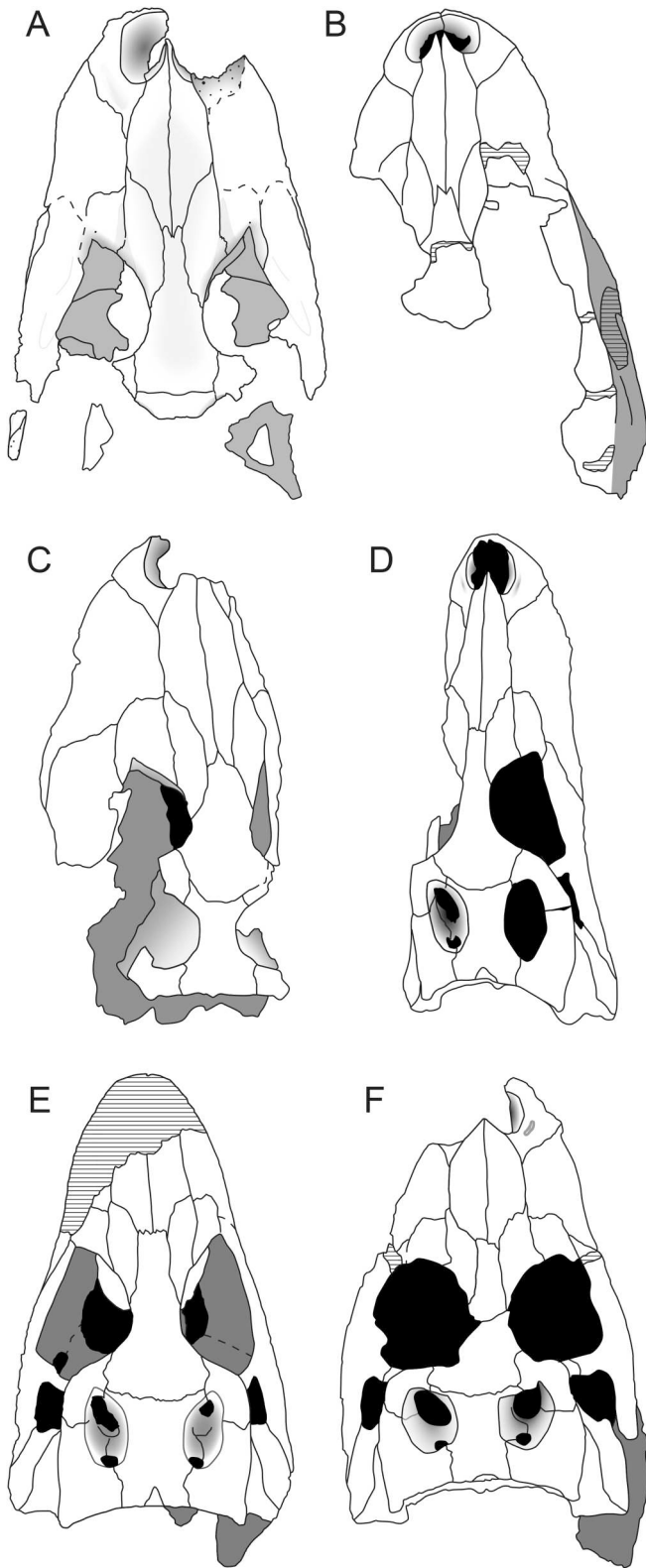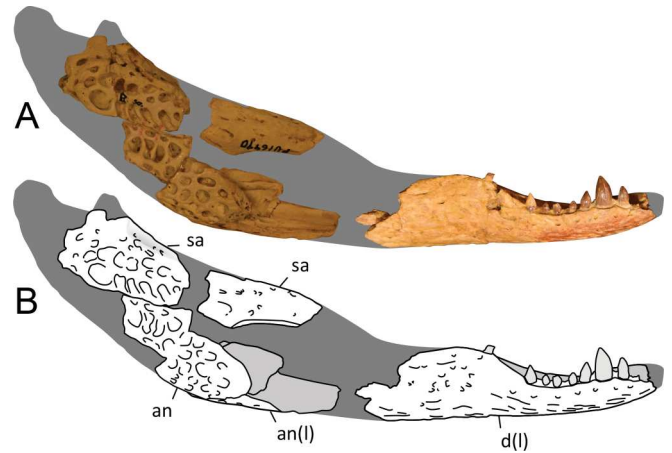

FIGURE 9. Interpretive line drawings (dorsal view) of alligatorid taxa recovered as close relatives of *Ahdeskatanka russlanddeutsche* by the most parsimonious trees in this study. **A**, *Ahdeskatanka russlanddeutsche*, YPM VPPU.016990 holotype specimen. **B**, *Allognathosuchus polyodon*, AMNH 6049. **C**, *Allognathosuchus wartheni*, YPM VPPU.016989. **D**, *Procaimanoidea utahensis*, USNM 15996 holotype specimen. **E**, *Procaimanoidea kayi*, CM 9600 holotype specimen. **F**, *Arambourgia gaudryi*, MNHN QU17155 holotype specimen.

obscures part of the alveolus itself and a small region of the premaxilla. Alveolar positions 1–3 and five are smaller and roughly similar in size with occlusal marks present lingual to the first premaxillary alveolus, the juncture of the second and third alveoli and third and fourth alveoli. These marks, formed by dentary teeth 1–3 respectively, suggest an overbite. A large pit is preserved lingual to the junction of the last premaxillary and first maxillary alveoli—this structure intersects the premaxillary–maxillary suture as is common to alligatoroids and was likely created by occlusion of the fourth dentary tooth. A large diastema is preserved between the occlusal marks formed by the presumed third and fourth dentary teeth.

Maxilla—The maxilla is both short and broad contributing to the blunt snout in this species (Fig. 6). On the left side the dorsal surface is perfect save the posteriormost portions of the element whose sutures are somewhat obscured. The medial margin of the right element, pushed ventrally along its sutural contact with the nasal, experienced slight crushing. The element's dorsal surface indicates a relatively smooth, flat surface free of bosses, ridges, or other protuberances. The anterolateral margin forms a point that is confluent with the obliquely trending premaxillary–maxillary suture. Medially, the maxillae bear linear margins contacting the nasals and prefrontals for a very short distance—the length of contact between the maxilla and nasal is shorter than closely allied alligatorids (Fig. 9). Posteriorly, the element bears three processes whose lengths increase from medial to lateral. The medialmost process is diminutive and at the midpoint of the anterior lacrimal margin. The intermediate process is moderately long and interposed between the anterior lacrimal and jugal. The dorsoventrally short, but anteroposteriorly long, lateralmost process of the maxilla trends along the lateral face of the jugal meeting the element at a ventrally bowed suture (Fig. 7). Preservation is perfect on the right but separated from the main body of the element via a large crack on the left. Ventrally, the element experienced dorsoventral compression and cracking separating the corresponding sides at the anterior midline where they formed the posterior margin of the incisive foramen. In ventral view, the posteriormost element terminates anterior to the lower temporal bar and contacts the jugal. Posteromedial to the final alveoli, the maxilla broadly

separates the ectopterygoid from contacting the maxillary toothrow. On the lateral surface of the maxilla, just superior to the toothrow, is a line of transition from the vertical orientation of the lateral surface of the maxilla to a lateral orientation—this area is confluent with the same transitional morphology present on the premaxilla (Fig. 7). Within this structure is a substructure, represented in the figure as a shaded region corresponding to the surface lateral to maxillary alveoli 9–13, that dips ventromedially relative to the generally lateral surface of this structure.

Each maxillary hemiarch bears 13 teeth with apices varying from conical mesially to conical or globular distally (Fig. 7). All teeth and alveoli are roughly circular in cross section, bear smooth mesiodistal carina, and basiapical striations. Alveoli grow progressively larger from the first to fourth position, which is the largest in the maxillary arcade, and then smaller to the point of the sixth alveolus. The seventh position is large relative to the alveoli flanking it mesiodistally. Alveoli then grow larger from the eighth to twelfth positions, and the thirteenth position is roughly the same size as the tenth position. The distal four maxillary teeth bear blunt crowns being nearly as wide as they are long and mesiodistal measurements of the crowns indicate nearly identical sizes among the sides. Crowns 10–13 on the left side measure 3.5, 6, 7, and 3 mm, whereas crowns 11–13 on the right side measure 5.5, 7, and 3 mm. Comparison to closely related species indicates that the great difference in size between the penultimate and ultimate tooth in the maxillary toothrow is autapomorphic. In occlusal view, the toothrow bearing the mesialmost six maxillary teeth preserves a gentle buccal curve transitioning to a gentle lingual curve posterior to this point. Corresponding to the regions bearing the largest alveoli are lateral expansions of the maxilla with an intervening medial constriction corresponding to relatively smaller alveoli. Occlusal marks lingual to the second and third, fifth and sixth, and seventh and eighth alveoli indicate an overbite.

Dentition—This specimen includes both socketed and loose teeth with the latter discussed here. Of the 10 loose teeth, nine preserve conical crowns with apices ranging from high to relatively low, and the remaining one preserves a root only (Fig. S1). All crowns preserve smooth mesiodistal carina and basiapical striations. Most teeth preserve a slight re-curve, presumably lingually or distally oriented. Owing to their relatively gracile morphology, they do not represent posterior portions of the dental series but precise identification is impossible.

Nasal—Preservation of both sides is very good (Fig. 6). Anteriorly, the premaxillary–nasal sutures are gently convex along the posteromedial margin of the dorsal processes and end at the posteromedial corner of the external nasal aperture where they make a lateral excursion along the posterior wall. Within the aperture, the nasals end in points that bisect the structure approximately halfway along its anteroposterior length. These points form the posteromedial and medial margins of the aperture. At mid-body, the elements are broad and whose lateral margins, in contact with the maxillae for a very short distance, are nearly parallel. Posterolaterally, the nasals form sutures with the prefrontals whose concavity faces posterolaterally. The posteriormost points of the nasals contact the frontal at a complex W-shaped suture similar to *A. polyodon* but with shorter lateral prongs (Fig. 9). In total, lateral margins are dorsally higher than the midline in the frontal plane. The impressed portion of the nasals is confluent with that of the midline portions of the prefrontals and frontal to form a large, indented, structure. *Allognathosuchus polyodon* preserves a similar indentation, includes the same elements, but does not reach as far posteriorly along the dorsal surface of the frontal as here.

Orbit—All orbital elements are preserved (Fig. 6). Preservation of the right orbit is better than the left and more accurately reflects the teardrop shape of the structure most closely

shared with similarly sized *A. wartheni* (YPM VPPU.016989), but relatively larger here (Fig. 9). The dorsal surface of the orbit is flush with the skull and margins are complete with the exception of the posterolateral margin formed by the lateralmost postorbital, and the postorbital bar, which is out of orientation with the skull table. The concave medial margin, formed by the frontal and posterior prefrontal, transitions into the concave anterior margin formed by the anterior prefrontal and lacrimal. The anterolateral edge of the orbit projects into the posterior lacrimal as a large, anteriorly oriented, v-shaped indentation similar to *A. wartheni*. Along the lateral border of the structure, the jugal is uplifted and contributes to the convex lateral orbital margin. Within the orbit, along the anterior face of the postorbital the lateral face of the frontal, prefrontal, and posterior lacrimal a groove is present and confluent among the elements. This groove ends at the pointed anterior margin of the orbit between the lacrimal and jugal (Fig. 7). Palpebrals are not preserved.

Prefrontal—Prefrontals, including their margins and sutural contacts are completely preserved (Fig. 6). The dorsal surfaces of the elements dip ventrally from lateral to medial and this ventrally impressed region is confluent with that of the nasals and frontal. Laterally, a triangular indentation trends along the prefrontal–lacrimal sutural contact (Fig. 7). The anterior frontal and posterior nasals separate the prefrontals in the midline and the acute anterior tip of the prefrontal exceeds that of the lacrimal—all closest relatives share these character states with *A. russlanddeutsche*, but the length of the prefrontal anterior to the lacrimal is greater here (Fig. 9). The lateral margin is best preserved on the right side and indicates a short convex suture with the posteromedial lacrimal which transitions into a long, linear sutural contact with the medial aspects of the lacrimal and maxilla. Although similar to *A. gaudryi* and *P. utahensis*, the prefrontal and the associated sutural contacts are proportionally longer (Fig. 9). Anteromedially, the prefrontal meets the nasal at a mediolaterally trending suture from anterior to posterior. The medial margins of the prefrontals meet the frontal at a sublinear, parallel sutural contact. This suture transitions posteriorly into a mediolaterally trending contact that ends in acute points at the orbital margin. The posterolateral margin of the prefrontal is concave and forms the anteromedial margin of the orbit. A groove is present within the orbit, along the lateral face of the element, and is confluent among the elements forming the medial and anterior margins of the orbit (Fig. 7). A small foramen, possibly for the conveyance of a branch of the ophthalmic division of CN V, is present on the posterolateral aspect of the element within the orbit and is most clear on the left side. Ventrally, the prefrontal pillar is not preserved.

Lacrimal—Both lacrimals are preserved and sutural contacts are completely traced using information from both sides. The anterior left lacrimal preserves a perfect contact with the maxilla and the right element preserves perfect contacts with the prefrontal and jugal (Fig. 6). The right element lies ventral to the maxilla and slight cracking is present along its anterior margin. Both sides demonstrate a very short, blunt posterior process of the maxilla projecting into the anterior face of the lacrimal and most closely resembles the morphology of *A. gaudryi* and species of *Procaimanoidea* (Fig. 9). This suture is complete on the left side, but accurately inferred on the right, revealing a posteriorly convex anterior suture that meets the lateral prefrontal at a short but acute point. The medial contact with the prefrontal is linear until the concave posteriormost extent of the element—similar to *A. gaudryi* and species of *Procaimanoidea*. The posterior margin, shaped like an inverted V, forms the anterior margin of the orbit and is similar to *A. wartheni*, although the rest of the element's dorsal surface including relative length and shape of sutures is distinct (Fig. 9). The lateral contact with the jugal is convex posteriorly and linear anteriorly. Along

the medial face of the jugal, a post-preparation break of the fossil disarticulated the posterior left portion of the element from its body. Posteriorly, at the anteriormost margin of the orbit, the lacrimal foramen is most clear on the left side. Dorsoventral compression of the right element in the region of the maxilla renders the anterior and lateral portions of the element ventral to the prefrontal.

Jugal—Both sides are preserved but a post-preparation break renders the left element disconnected from the maxilla at their sutural contact (Figs. 6, 7). The right side experienced slight damage anteriorly but the sutural contact with the maxilla is accurately traced. Dorsally, the medial contact with the lacrimal is linear for a short distance, transitions into a laterally convex structure posteriorly then intersects the lateral margin of the orbit approximately halfway along its length. The anterior margin is blunt, almost equal to the lacrimal in its anterior extent, and differentiates *A. russlanddeutsche* from close relatives (Fig. 9). Laterally, the element contacts the maxilla at a broad, ventrally convex suture that trends posteriorly with a ventral dip. The element is robust in lateral view, especially so in comparison to similarly sized *A. mississippiensis*. The element's contribution to the lower temporal bar and lateral margin of the obit are tall resulting in the great depth of the posterior upper jaw. The slender postorbital bars have been pushed ventrally—only the jugal's contribution to the structure is preserved and hinders character coding for the superior part of the bar. It is inset from the lateral surface of the jugal, best preserved on the right side, and welded to the body of the ectopterygoid on the left. Along the medial face of the element, anterior to the postorbital bar, the medial jugal foramen for the passage of the jugal branch of the maxillary division of CN V is small. A small fragment of the posteriormost jugal process along the quadratojugal demonstrates the quadratojugal–jugal suture on its medial and posterosuperior face (Fig. 8H).

Quadratojugal—Both sides are missing, but sutural marks on the jugal along the medial face of the lower temporal bar indicate that the quadratojugal sends an anterior process. Due to incomplete preservation of this region, the relative length of the anterior process along the lower temporal bar is indiscernible and unscored in the phylogenetic analysis.

Quadrate—Part of the ventral, right quadrate is preserved (Figs. 6, 8J). The ventral surface of the quadrate ramus demonstrates attachment scars in the form of modest crests for the attachment of the adductor mandibulae posterior muscle. The anteroventral portion of this fragment preserves the posterior margin of the trigeminal foramen (Fig. 8J). This margin is confluent with a groove trending away from the foramen for the conveyance of the mandibular ramus of CN V.

Skull Table—Most skull table elements are preserved, but posterior elements are not in contact with their anterior counterparts (Fig. 6). The supraoccipital is not preserved. The dorsal surface of the skull table is planar but as the margins of the structure are not confluent, many characters describing the gross morphology of the posterior skull table are unscored in the matrix. Although the anterior margins of the supratemporal fenestrae are preserved, the supratemporal fossae in their depths are not.

Supratemporal Fenestra—Both fenestrae are preserved but best appreciated on the right side (Fig. 6) and differentiated from close relatives via shape and elemental contribution (Fig. 9). The anteromedial margin is broadly concave, exclusive of a fossa, and formed by the parietal. The postorbital forms the bluntly pointed anterior margin. Among the preserved margins, the skull table elements gently grade into the fenestrae and do not overhang the rim of the structure. However, due to an incomplete medial margin, characters describing this region are unscored.

Frontal—The element is completely preserved. Some transversely oriented cracking is present in its contribution to the skull table (Fig. 6). Anteriorly, a constriction of the element between the prefrontals ends in a complex sutural contact with the nasals. This suture is trident shaped anteriorly, and whose lateral prongs are long and whose midline prong is very short —this morphology is similar to *A. polyodon* but distinguishable via shape and relative lengths of processes (Fig. 9). The lateral edges of the frontal form the broadly concave medial margins of the orbit (Figs. 6, 7). The relatively wide frontal in this region is most similar to species of *Allognathosuchus*, but distinguishes the taxon from other close relatives (Fig. 9). The element is ventrally impressed along the midline and is confluent with the impressed regions of the prefrontals and nasals. The element is exclusive of crests, ridges, or prominent depressions in the area of the orbits. Posterolaterally, the element makes contact with the postorbitals at a nearly anteroposteriorly linear suture. The posterior margin forms a roughly linear sutural contact with the parietal immediately anterior to the supratemporal fenestrae and differentiates the taxon from closely related species in this analysis that have concavo/convex sutures (Fig. 9). The frontal meets the postorbital and parietal at a three-way sutural contact that is entirely on the skull table and does not enter the supratemporal fenestra. Ventrally, adhered bone in the region of the braincase obscures the frontal's contribution to this structure.

Postorbital—Preservation of anteromedial portions of both postorbitals demonstrate that they form the posterior margin of the orbit and the anterior margin of the supratemporal fenestra (Fig. 6). Ventrally, the postorbital forms a small portion of the dorsomedial postorbital bar. Dorsally, they make broad contact with the frontal along an anteroposteriorly oriented suture— the linearity of which distinguishes the taxon from close relatives (Fig. 9). Immediately posterior, and confluent with the sutural contact with the frontal, the postorbital meets the parietal at a very short, linear suture and contacts the anterior margin of the supratemporal fenestra.

Parietal—The anteriormost parietal is preserved between the supratemporal fenestrae (Fig. 6). Anteriorly, the element contacts the frontal at a nearly linear, mediolaterally trending suture. Laterally, the element meets the postorbital at a short, anteroposteriorly linear suture intersecting the anterior margin of the supratemporal fenestra. Between the supratemporal fenestrae, the element is constricted and forms part of the anteromedial margin of the structure. Posterior to this the element is broken, exposing the inner surface of the parietal in the transverse plane. The ventrolateral margin of the element preserves bilateral canal-like structures that may represent the anteriormost portions of the parietal sinus, or canals for communication with the pneumatic system. Ambiguity renders these structures unscorable in the matrix. Ventrally, the element contributes to the dorsal surface of the braincase through the preservation of a fossa, likely for the posterior cerebrum.

Squamosal—Parts of both elements are preserved (Figs. 6, 8). Both the longer posterolateral left and shorter posterolateral right fragments preserve the dorsal margin of the external auditory meatus and the posterior squamosal groove for the external ear musculature (Fig. 8F, G). Posterior portions of the dorsal and ventral rims of the squamosal groove are parallel, but due to incomplete preservation, this character state is not scored in the matrix. Comparison to taxa with horn-like squamosals indicates that this species preserves enough of the posterolateral squamosals to code the character state as horizontal rather than upturned—the element is dorsoventrally short in lateral view (Fig. 8F, G).

Suborbital Fenestra—Post-mortem diagenesis altered the margins of the suborbital fenestrae, description is via aggregate from both sides, and some characters describing this region are unscored in the phylogenetic analysis. Although displaced from their presumed orientation in life, the maxillary ramus of the

ectopterygoid clearly contributes to the concave lateral margin of the fenestra, as does the pterygoid ramus of the respective element which contributes to the straight posterolateral margin and exceeds the former's length (Fig. 6). The posterior margin is incomplete owing to the poor preservation of the pterygoids and palatines. Medially, the palatine forms the concave medial margin and the maxilla forms the anterior margin. The state of the palatine–maxillary suture relative to the anteromedial margin of the suborbital fenestra cannot be determined due to alteration of the palate in this area.

Vomer—The element is likely preserved but is indistinguishable from the maxilla in the region of separation at the midline. Poor preservation results in an unscorable character at the point of the premaxillary–maxillary suture. Posterior to this point of separation, the maxillae and palatines entirely obscure the vomer. Phylogenetic comparison to related species indicates that exposure of the vomer on the palatal surface of the upper jaw is extremely unlikely.

Palatine—The palatines are preserved but crushed and pushed dorsally against other elements in the region, and are missing their posteriormost margins (Fig. 6). The anterior sutural contact with the maxilla ends in a broad, blunt point extending approximately five alveoli anterior to the suborbital fenestrae. Although the structure is complete, a dashed line represents the anterior sutural contacts with the maxilla due to alteration hindering precision in the figure. Anterolaterally, the element forms subparallel sutural contacts with the maxilla that obliquely trend as they approach the suborbital fenestrae. The elements form the smooth, concave medial margins of the suborbital fenestrae exclusive of lateral projections anteriorly—incomplete preservation of the element hinders character coding posteriorly. At mid-body the elements have been pivoted toward the right rendering a small portion of the right palatine visible in dorsal view through the orbit. It is likely that this distortion also accounts for the nonlinear midsagittal suture connecting the elements and hinders tracing the contact along its length. Morphology is most similar to *Procaimanoidea kayi*, but differentiated via the greater relative width of the structure between the suborbital fenestrae and the relatively longer anterior process.

Ectopterygoid—Both ectopterygoids are preserved and missing only the ventralmost tips (Figs. 6, 7). The elements appear to have a slight medial rotation from their presumed orientation in life. As best indicated on the left side, the short maxillary and jugal rami of the ectopterygoid end in blunt points. Reconstruction of life position indicates that the former forms part of the lateral margin of the suborbital fenestra, does not exceed 2/3 of the margin, and has no intervening process of the maxilla separating it from direct contact with the fenestra. The jugal ramus does not contribute to the slender postorbital bar.

Pterygoid—Two pieces of the left pterygoid are preserved. The first piece, sutured to the left ectopterygoid, forms part of the linear posterolateral margin of the suborbital fenestra and demonstrates no ectopterygoid–pterygoid flexure in this mature individual (Fig. 6). The position of the second piece, an isolated lateroventral pterygoid flange (Fig. 8I) is indicated in the figure by a red line corresponding to a complementary red line on the left ectopterygoid (Fig. 6A). This fragment preserves sutural marks indicating that the ectopterygoid ends about 0.5 cm from the ventral tip of the element.

Mandible—Isolated posterior mandibular elements are preserved (Fig. 8A–E). Morphology of the type specimen, YPM VPPU.016990, combined with the most well-preserved dentary specimen referred to the species, YPM VPPU.016902, creates a holistic appraisal of the mandible. The jaw is reconstructed (Fig. 10) as short with a tall jaw joint and long, robust mandibular symphysis. Ornamentation of the lateral surface of the mandible is pronounced posteriorly and dorsally with rugose lineations anteroventrally.

Dentary—An isolated fragment of the dentary is preserved (Fig. 8E). Deeply pitted ornamentation present on one surface indicates it is from the lateral aspect of the dentary—the preserved alveolar margins represent the buccal surfaces. The ventral aspect of this fragment preserves a longitudinal trench for the Meckelian groove.

Surangular—Incomplete posterior right and left surangulars are preserved (Fig. 8A, B). The lingual surface of the elements preserve the surangular's contribution to the simple, nearly linear sutural contact with the articular. The lingual foramen for the articular artery and inferior alveolar nerve pierces the surangular only and is separated from the suture by a very short distance. Along the anterosuperior surfaces of both sides the posterior end of a broad, flat shelf for the attachment of adductor mandibulae externus superficialis is preserved. Both sides preserve a portion of the lateral margin of the articular fossa for the jaw joint, but preservation is best on the left side. Lateral to the articular fossa the element is dorsoventrally tall as is common among the closely related species of *Allognathosuchus*. Of the superior margin preserved by the left element, what remains is perfect including the area surrounding the glenoid fossa. Yet, the articular is not preserved and the character is unscored. It is unknown whether the surangular extended to the dorsal tip of the glenoid fossa, but comparison to closely related species suggests it did. Another piece tentatively identified as a portion of the right surangular (Fig. 8D) with the dorsal margin of the external mandibular fenestra, may indicate that this specimen had a relatively large fenestra as is common among its closest relatives and is included in the taxon's reconstructed lower jaw (Fig. 10). Characters describing the region of the external mandibular fenestra are unscored due to tentative identification and lack of context.

Angular—Both sides are preserved but incomplete (Fig. 8A, C). The right side preserves more of the lateral element including a modest portion of the floor of the mandibular fossa, external mandibular fenestra, and the posteriormost foramen intermandibularis caudalis. The left side preserves more of the medial element and also includes the posteriormost extent of the foramen intermandibularis caudalis. Judging by the right angular which preserves modest portions of both the external mandibular fenestra and the foramen intermandibularis caudalis, and based on proportions and extrapolation of the potential margins of the respective fenestrae, it is unlikely that the foramen intermandibularis caudalis was visible through the external mandibular fenestra, but was left unscored in the matrix. The depth of the inferolateral portion of the right angular relative to the proposed external mandibular fenestra suggests a relatively small fenestra here. The right angular and surangular meet at an area denoted by two small red lines drawn during excavation (Fig. 8A). The combined morphology of the two elements suggests an elevated jaw joint and a dorsoventrally deep posterior lower jaw as is common to the closely related species of *Allognathosuchus*.

REFERRED SPECIMENS

YPM VPPU.030620

This specimen represents a small, complete left premaxilla referable to *Ahdeskatanka russlanddeutsche* from this locality (Fig. 11A). Comparison to the holotype indicates an individual of similar size with a shared pattern of ornamentation on the dorsal surface. Morphology shared with the holotype includes proportion, shape, and size of the external nasal aperture and incisive foramen. In both this specimen, and the holotype, the lateral margin of the external nasal aperture is straight and a modest indentation posterolateral to the structure is preserved. The palatal lamina of the element bears sutural marks along
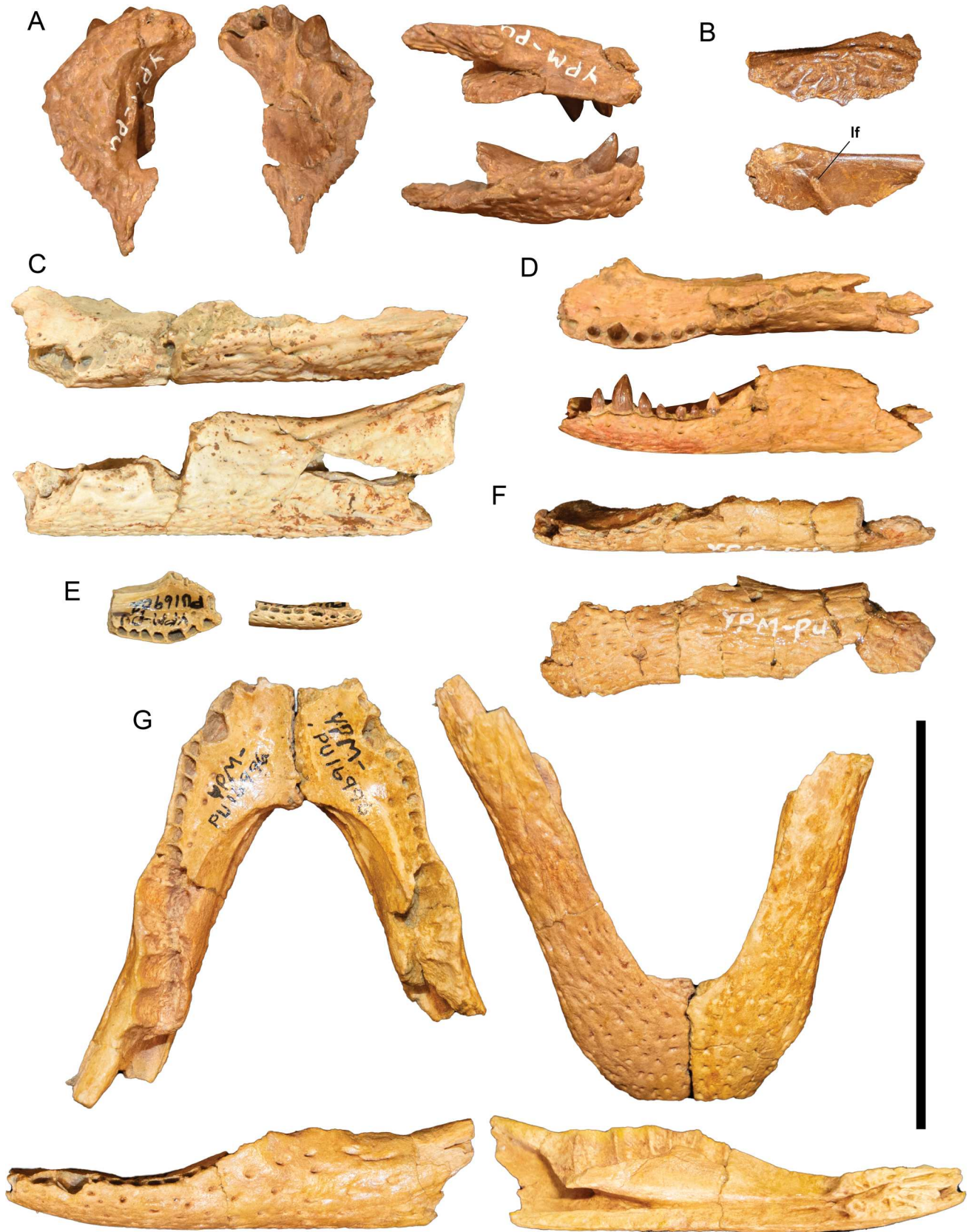
FIGURE 11. Elements referable to *Ahdeskatanka russlanddeutsche*. **A**, YPM VPPU.030620, left premaxilla in dorsal (furthest left), ventral (left), medial (top right), and lateral (bottom right) views. **B**, YPM VPPU.030623, left surangular in lateral (top) and medial (bottom) views. **C**, YPM VPPU.016902, (large) left dentary in dorsal (top) and lateral (bottom) views. **D**, YPM VPPU.016902, (medium) right dentary in dorsal (top) and lateral (bottom) views. **E**, YPM VPPU.016902, (small) right dentary in dorsal (top) and lateral (bottom) views. **F**, YPM VPPU.030621, dentary in dorsal (top) and lateral (bottom) views. **G**, YPM VPPU.016996, dentaries in dorsal (top left) and ventral (top right) views. Left dentary in lateral (bottom right) and medial (bottom left) views. Scale bar equals 5 cm.

the medial surface where it met the maxilla. In agreement with morphology preserved here and in the holotype, the maxilla forms the posterior margin of the incisive foramen. Both dorsally and ventrally, the trend of the premaxillary–maxillary sutural surfaces are shared with the holotype, as are the proportions of the dorsal process of the premaxilla. Ventrally, the specimen preserves five alveoli with complete teeth in positions three and four and a root in position five. Shared proportions are evident with the fourth position being larger than the similarly sized remaining positions. Poor preservation of premaxillary teeth in the holotype hinders comparison with this specimen. The occlusal mark pattern is shared but this specimen preserves an indentation lingual to the fourth and fifth alveoli whereas diagenetic alteration is present in this region of the type.

YPM VPPU.016902

This catalog number consists of eight loose teeth, one bone fragment, and three dentaries of different sizes from the White Butte Site. The dentary specimens represent different individuals and relative to the other two, the largest is poorly preserved.

Eight loose teeth and a single bone fragment are included in this lot. Whether these teeth are associated with one of the specimens in the lot or gathered via surface collection is unknown, but they were likely associated with an individual approximately the same size as the largest specimen in this lot. Six teeth are conical with smooth mesiodistal carina and basiapical striations of the enamel. These teeth have a slight recurve that is presumed to trend posteriorly. Two of the teeth are bulbous with very short crowns and basiapical striations. The bone fragment is small and unidentifiable to element.

The smallest of the dentary specimens consists of an anterior right dentary (Fig. 11E). Eight alveoli are preserved, seven are complete, the first alveolus is missing its buccal margins, and no teeth are preserved. All alveoli are roughly circular and the fourth alveolus is the largest among the preserved arcade. The dentary symphysis is anteroposteriorly longer than it is tall and in dorsal view extends to the seventh alveolus (Fig. 13C). Posterior to the dentary symphysis, a sharp ridge separates the dorsal surface of the dentary from the lingual surface.

The mid-sized specimen consists of a left dentary of which the posteriormost extent is missing (Fig. 11D). Fifteen alveoli are preserved but the buccal margins of alveolar positions 1–2 and lingual margins of positions 11–15 are missing. The first alveolus is large, the second and third are smaller and similar in size, the fourth alveolus is the largest in the arcade, 5–11 are small and nearly the same size, 12 is large, 13 is very large, 14 and 15 are smaller, 16 and 17 are large. Alveolar positions 3–9 and 11–12 preserve conical teeth with smooth mesiodistal carinae and rugose basiapically oriented striations of the enamel. The fourth tooth bears a slight distal recurve. When viewed laterally, two regions are uplifted along the toothrow. The anterior uplift centers on the fourth alveolus and the posterior as a pronounced dorsal ridge beginning at the tenth alveolus (Fig. 13B). Medially, this specimen bears a sharp ridge posterior to the dentary symphysis and marks the transition from the dorsal surface of the element to the lingual surface—similar to the smallest specimen in this lot. The robust dentary symphysis extends to the seventh alveolus (Fig. 13B).

The largest specimen consists of a fragmentary left dentary (Fig. 11C). The anteriormost toothrow and symphyseal region is not preserved and matrix obscures morphology at midbody and posteriorly. Thirteen alveoli are preserved but poor preservation hinders their identification by position in the dental arcade. Like the midsized specimen in this lot, the anterior alveoli are considerably smaller in diameter than their posterior counterparts. The anteriormost alveoli are missing their buccal margins and posterior alveoli are missing their lingual margins. Comparison of

the uplifted portion of the lateral margin indicates that this is the area around the 10th–15th alveoli. The pattern of sculpturing is similar to the other two dentaries in this lot.

The dentaries share morphology and represent an ontogenetic series. Shared alveolar proportions and symphyseal and Meckelian groove morphology indicate that the smallest and midsized dentaries in this lot represent the same species. Proportions of alveoli and a pronounced posterior dorsal ridge of the toothrow are shared between the midsized and largest specimens in this lot. Additionally, all three dentaries share a similar pattern of ornamentation and evidence here indicates an ontogenetic component and more pronounced ornamentation at larger body sizes (Clarac et al., 2015; de Buffrénil, 1982; de Buffrénil et al., 2015).

YPM VPPU.030621

This specimen was recovered from an unknown site within the South Heart Locality by a 1960 Princeton University excavation. One fragmentary left dentary with 13 alveoli is included in the lot (Fig. 11F). The posterior four alveoli preserve buccal margins only. The largest anterior alveolus is presumed to represent the fourth position and the dentary symphysis extends to the juncture of the seventh and eighth alveoli. On the medial surface of the element, posterior to the dentary symphysis, a ridge separates the horizontal dorsal surface from the vertical lingual surface at a nearly right angle. Curvature and proportions of the preserved toothrow are similar to species of *Allognathosuchus* and likely represents *A. russlanddeutsche*.

YPM VPPU.030623

This specimen was recovered from the South Heart Locality by a 1960 Princeton University excavation—the site is unknown. One posterior left surangular from the region inferior to the jaw joint is preserved (Fig. 11B). This element is referable to *A. russlanddeutsche* due to the presence of a lateral boss inferolateral to the jaw joint, similarity in the pattern of sculpturing on the lateral surface, and the lingual foramen entirely on the surangular.

YPM VPPU.016996

YPM VPPU.016996 consists of small, edentulous left and right mandibular rami in articulation (Fig. 11G) from the White Butte Site. Estes (1988) suggests this lot consists of right and left dentaries, an isolated left dentary, and a left premaxilla. The authors believe YPM VPPU.030625 or YPM VPPU.030621, which include partial left dentaries, and YPM VPPU.030620, a left premaxilla, may have been included in this lot when originally assigned.

Preservation is three-dimensional and the left dentary preserves more of the element than the right side. Similar to the YPM VPPU.016902 dentaries, sculpturing of the elements consists of pitting on the dorsolateral surface and transitions into long, linear furrows ventrally. Also shared with the YPM VPPU.016902 dentaries, posterolateral to the dorsal exposure of the symphysis, a sharp ridge separates the dorsal surface of the dentary from the lingual surface. In dorsal view, the dentary symphysis is long and jagged and extends to the eighth alveolus (Fig. 13E). When disarticulated, the sutural surface of the symphysis is more than twice as long as it is tall. The medial surface of the element demonstrates sutural marks for the juncture with the splenial, which is not preserved.

The left element best preserves the edentulous toothrow. Margins of anterior teeth are damaged crownward, positions 5–10 are perfect and positions 11–18 are missing their buccal margins. The first alveolus is large, the second and third are smaller and similar in size, the fourth is very large, 5–11 are small and nearly the same size, 12 is large, 13 is very large, 14
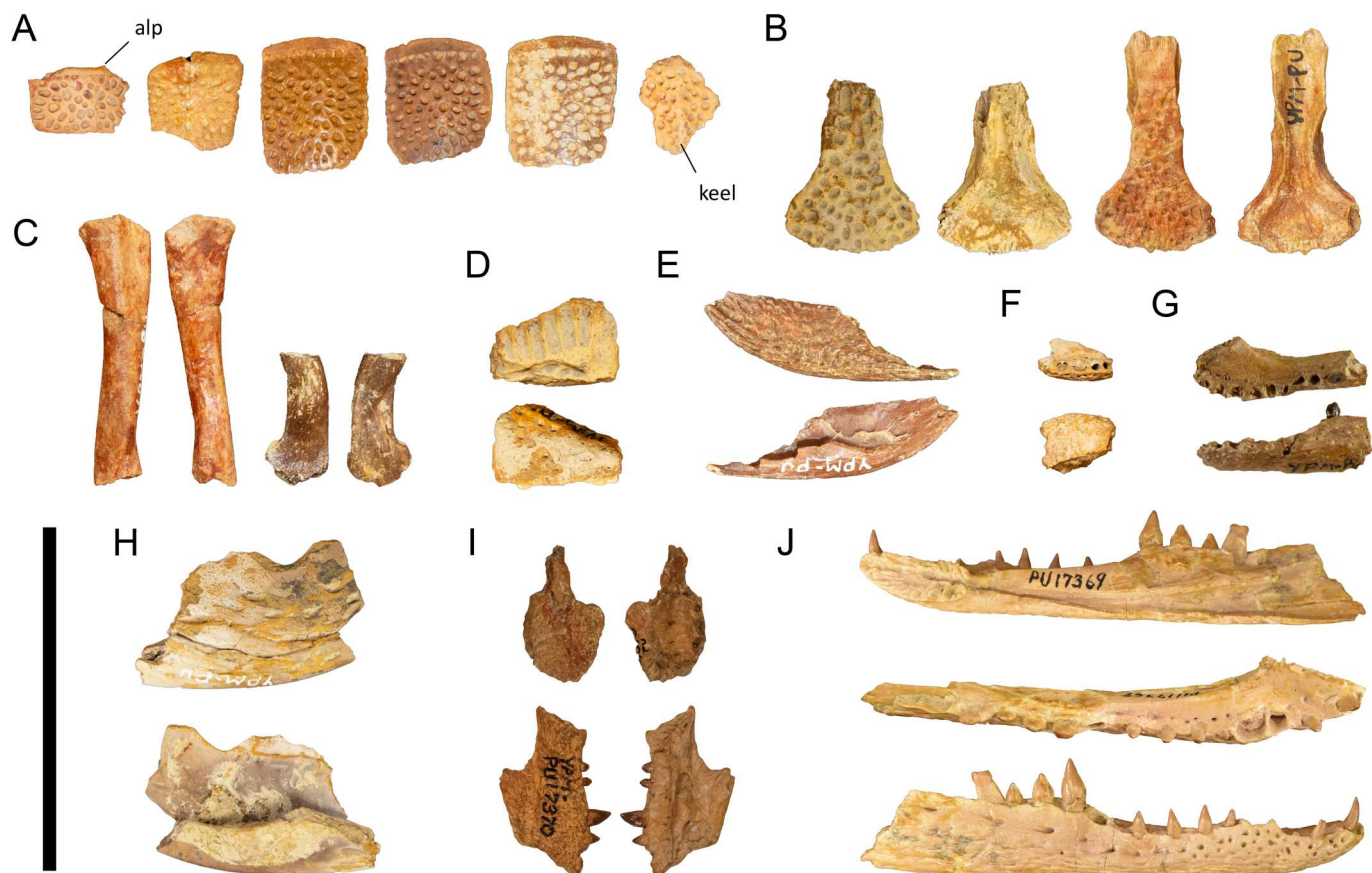
FIGURE 12. Additional crocodylian elements from the South Heart Locality. **A**, YPM VPPU.030624, selected osteoderms in dorsal view. **B**, YPM VPPU.030624, frontals in dorsal and ventral views. **C**, YPM VPPU.030624, femora. **D**, YPM VPPU.030622, right dentary fragment in medial (top) and lateral (bottom) views. **E**, YPM VPPU.030622, right angular in lateral (top) and medial (bottom) views. **F**, YPM VPPU.030622, maxillary fragment in ventral (top), dorsal (top) views. **G**, YPM VPPU.030622, right dentary in dorsal (top) and lateral (bottom) views. **H**, YPM VPPU.030622, left angular fragment in lateral (top) and medial (bottom) views. **I**, YPM VPPU.017370, right maxilla (top) in dorsal (top left) and ventral (bottom left) views and left maxilla (bottom) in dorsal (bottom left) and medial (bottom right) views. **J**, YPM VPPU.017369, right dentary in medial (top), dorsal (middle), and lateral (bottom) views. Scale bar equals 5 cm.

and 15 are intermediate in size relative to their mesial and distal counterparts, and positions 16–18 are large. The right element preserves morphology in agreement with the left side but ends at alveolar position 16. Relevant to the phylogenetic analysis, the fourth and thirteenth alveolar positions are the largest in the anterior and posterior toothrow respectively. In lateral view, two regions of uplift are present along the toothrow. The anterior uplift centers on alveolar positions 3–5 and the posterior uplift begins its incline at position 10 (Fig. 13E). These features, shared with YPM VPPU.016902, suggest the same species.

The *A. russlanddeutsche* holotype specimen is strikingly similar in size to this mandible and preserves an upper jaw with 18 alveoli per side of the hemiarcade—the left hemimandible, which preserves the complete mandibular hemiarcade, has the same number. Although VPM-VPPU.016990 does not preserve a complete dentary, phylogenetic bracketing suggests a tentative referral to *A. russlanddeutsche* through reference to allied species that do preserve this element.

ADDITIONAL SPECIMENS FROM THE LOCALITY

YPM VPPU.030622

This lot consists of various incomplete elements recovered from the South Heart Locality by a 1960 Princeton University

excavation—the site is unknown and the elements are not referable to species.

Less completely known specimens will be discussed here with elaboration on the more completely known angular in the following paragraph. Forty teeth in various states of preservation are included in this lot. All teeth are small, some with tall crowns and smooth mesiodistal carinae, others with bulbous, low crowns. Comparison to more complete tooth-bearing elements from the locality indicates the breadth of morphology preserved by teeth in this lot represents multiple species. Also included is one very small maxillary fragment with four alveoli, two of which bear broken crowns (Fig. 12F). One larger, incomplete left angular preserves the mid-body of the element (Fig. 12H). The lateral surface is deeply sculptured. Medially, the mandibular fossa and the fossa's medial lamina are preserved. A fragment of dentary preserves the buccal margins of seven, similarly sized alveoli (Fig. 12D). Matrix covers part of the pitted lateral surface.

A small, right angular preserves the element's mid-body (Fig. 12E). Small parts of the anterior, posterior, anteromedial, and anterolateral margins are not preserved. Medially, the mandibular fossa is preserved and curvature of the anterodorsal surface may indicate the chipped margins of the external mandibular fenestra. Curvature of the element's ventral surface, forming the posteroventral angle of the mandible, does not match that of the *A. russlanddeutsche* type. Alteration of the

element in the *C. mylnarskii* type prohibits comparison and referable specimens do not preserve this element. Comparison to *Borealosuchus formidabilis* from the Paleocene age Wannagan Creek site of western North Dakota (Erickson, 1976) indicates similarities in proportions of margins and sculpturing with anteroposteriorly linear furrows along the inferior margin of the element.

YPM VPPU.030624

This lot consists of a number of elements belonging to small individuals collected in 1960 by a Princeton expedition to the South Heart Locality—no site information is associated with these specimens. Two small, partial left femora preserve distal and proximal joint surfaces and parts of the shafts, respectively (Fig. 12C). Twelve dorsal osteoderms are included of which six are complete or nearly complete and figured here (Fig. 12A). They are gently concavo/convex when viewed in the transverse plane and one has a keel while the others do not. Four of the five osteoderms preserving nearly complete margins are roughly square. Another is rectangular with a mediolaterally long axis and preserves a small part of an anterolateral process as found in species of *Borealosuchus*. Differences between these elements indicate a minimum of three species. The keeled osteoderm specimen bears morphology similar to species of *Allognathosuchus*, and may represent *A. russlanddeutsche*, the rectangular specimen with the anterolateral process may belong to a species of *Borealosuchus*, and the square, unkeeled specimens may belong to *C. mylnarskii*.

Among cranial elements, two loose teeth are included demonstrating crowns with tall apices, basiapical striations and smooth mesiodistal carinae. Two frontals (Fig. 12B), of similar size represent the same species. These elements collectively constitute the entire element and its sutural surfaces. The tan specimen, missing its anteriormost extent, preserves a slight dorsoventral indentation along the interorbital surface similar to both *C. mylnarskii* and *A. russlanddeutsche*. The larger, red-tan frontal also has a small indentation in this region. All sutural surfaces are complete. The anterior sutural contact, presumably with the nasals, is complex and W-shaped. The anterolateral sutural contacts, likely with the prefrontals, are nearly straight and trend mediolaterally from anterior to posterior. The interorbital region, which the element forms the gently bowed medial margin of the orbit, is thin mediolaterally. Posterolaterally, the sutural contacts, likely with the postorbitals, have a slight laterally oblique trend from anterior to posterior. The posteriorly convex suture with the parietal is similar to *C. mylnarskii*.

YPM VPPU.030625

YPM VPPU.030625 was collected by Princeton University in 1961 from an unknown site in the South Heart Locality. It represents a small individual preserving a partial left dentary with one tooth and 10 alveoli (Fig. 12G). The first alveolus is missing its lingual margin and the fourth alveolus is the largest among the preserved toothrow. The tenth alveolus preserves a complete, low crowned tooth with a smooth mesiodistal carina and rugose, basiapically oriented striations of the enamel—posterior to this point no morphology is preserved.

The dentary symphysis is preserved and its sutural surface is ovoid and twice as long as tall. The Meckelian groove intersects the posterior half of the sutural surface of the symphysis. Dorsally, the dentary's contribution to the symphysis extends to the juncture of the fifth and sixth dentary teeth (Fig. 13D). Although the splenial is missing, sutures representing the contact between the splenial and the dentary are preserved. Laterally, there are two uplifted regions of the toothrow corresponding to the region of the third to fifth alveoli and the region posterior to the seventh alveolus (Fig. 13D).

YPM VPPU.017370

Estes (1988:552) refers to this lot as "maxillary fragments, maxilla, and premaxilla" but these specimens represent the right and left maxillary fragments (Fig. 12I) from small individuals collected at the White Butte Site in 1961 by Princeton University. Preservation is good and coloration is variable between the specimens; the larger of the two fragments is darker and orange-tan in color; the smaller specimen is lighter and tinged with red-pink streaks.

The smaller of the two fragments represents an incomplete right maxilla (Fig. 12I) preserving five alveoli of uncertain position referred to here based on preserved position rather than definitive position along the maxillary toothrow. Among the alveoli, the first position preserves a broken crown in its depths —the presumed remainder of the crown is adhered to the element lingual to the toothrow. The third alveolus preserves a complete crown with a smooth mesiodistal carina and basiapical striations of the enamel. The fourth position preserves a broken crown. Deep neurovascular foramina are preserved lingual to the toothrow. Lingual to these foramina the palatal surface of the maxilla underlying the paranasal air sinus is intact, however, toward the midsagittal plane the palatal surface of the maxilla is missing exposing the dorsal and lateral walls of the nasal cavity. The posteromedial surface bears deep sutural marks tentatively identified as contacting the prefrontal or lacrimal in life.

Preservation does not allow for referral to species but this specimen appears to represent a region of the maxilla similar to that of the larger specimen in this lot. Reference to the larger specimen indicates that this fragment is missing portions of the posterior toothrow. Similarities in the shape of the toothrow, proportions of the alveoli, and contours of the sutural surface with the preorbital elements indicate that the maxillae in this lot represent the same species.

The larger of the two fragments is a posterior left maxillary fragment anterior to the contact with the preorbital elements (Fig. 12I). Eight alveoli are preserved, six of which are perfect. The positions of these alveoli cannot be determined but numbered based on preserved structures rather than definitive position along the toothrow in life. The eighth alveolus is missing parts of its medial and posterior margins and preserves an erupting tooth in its depths. Four conical teeth are present in alveolar positions 3–4 and 6–7. These teeth preserve a smooth mesiodistal carina with basicoapically oriented striations of the enamel and the tooth in the fourth position is the largest and bears a posterior curvature of the crown. Neurovascular foramina are preserved lingual to the toothrow. Lingual to these foramina, the palatal surface of the maxilla is missing and reveals the dorsal and lateral walls of a paranasal air sinus.

The dorsal side of the larger element preserves a narrow, medially trending furrow extending from the posterior to the anterior of the fragment. The medial edge of the element is linear and likely made contact with the corresponding left nasal. An extensive sutural surface preserved along the posterior element made contact with the prefrontal and/or lacrimal. Posterolaterally, the element ends in a projection tentatively identified as the jugal face of the maxilla whose posteriormost margin is missing.

It is not referable to *A. russlanddeutsche* based on the proportions of the posterior maxillary teeth in the larger specimen included in this lot. Although referred to *C. mylnarskii* by Estes (1988) comparison to the holotype is impossible due to poor preservation of the posterior maxillary toothrow. Crushing and displacement of bony surfaces in this region of the holotype makes reference based on proportions and the presence of the dorsal indentation unfeasible.

YPM VPPU.017369

This small, right dentary (Fig. 12J) collected at the White Butte Site preserves 15 alveoli, 13 of which are complete and
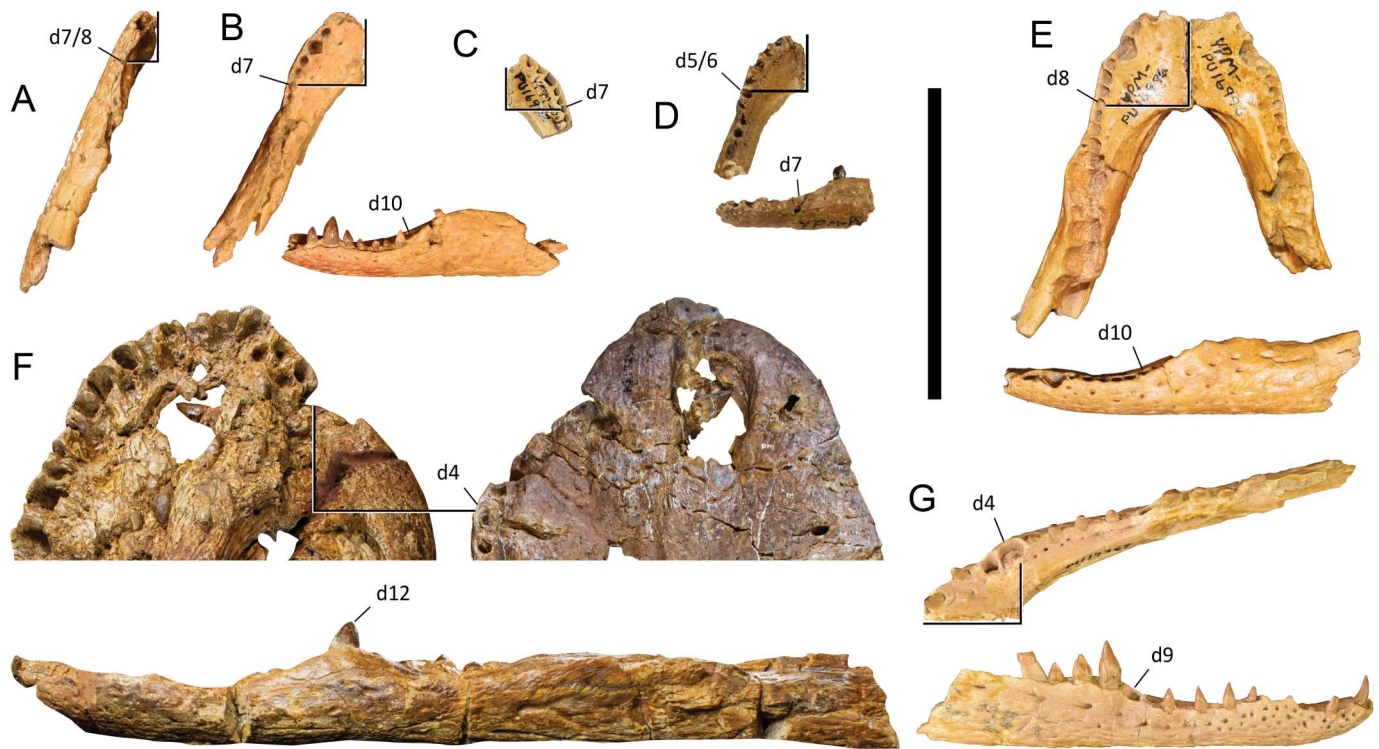
FIGURE 13. Comparison of mandibles from the South Heart Locality showing divergent morphology of the dentary symphysis and dorsal uplift of the posterior toothrow. **A**, YPM VPPU.030621, left dentary in dorsal view. **B**, YPM VPPU.016902, left dentary in dorsal (top left) and lateral (bottom) views. **C**, YPM VPPU.016902, right dentary in dorsal view. **D**, YPM VPPU.030625, left dentary in dorsal (top) and lateral (bottom) views. **E**, YPM VPPU.016996, left and right dentaries in dorsal view (top) and left dentary in lateral view (bottom). **F**, *Chrysochampsa mylnarskii* YPM VPPU.017258 holotype specimen, left dentary in ventral (top left), dorsal (top right), lateral (bottom) views. **G**, YPM VPPU.017369, right dentary in dorsal (top) and lateral (bottom) views. *C. mylnarskii* not to scale. Scale bar equals 5 cm.

the posteriormost two (alveoli 14–15) preserve only the buccal margins. Among the preserved alveoli, the fourth position is the largest in the anterior mandibular toothrow with the third and first positions being smaller and similar in size to one another. Alveoli 5–8 are small and similarly sized, 9 and 10 get progressively larger, 11 and 12 get progressively smaller. Alveolus 13 may be similar in size to 11 but the dorsally shifted tooth hinders interpretation of its margins. Alveolus 14 is likely the largest among the preserved posterior arcade and position 15 is missing both its lingual and posterior buccal margins.

Alveoli 1, 2, 5–8, and 10–13 bear teeth. Dorsal displacement of the tooth in the 13th alveolus exposes the root. All teeth are conical with a distinct apex, and preserve a smooth mesiodistal carina with basicoapically oriented striations of the enamel. In dorsal view, teeth are mesiodistally more expansive than they are buccolingually. Lingual and inferior to the toothrow neurovascular foramina are preserved. Although similarities exist between the proportions of the mandibular teeth between YPM VPPU.017370 and *B. formidabilis*, the evidence for confluent alveoli is very weak here and spacing of the anterior dentary alveoli differs.

When viewed laterally, there are two regions demonstrating uplift of the toothrow. These areas correspond to the third to fifth alveoli as well as the ninth alveolus and the region posterior to it (Fig. 13G). This is similar to *B. formidabilis* but in opposition to *C. mylnarskii* whose mandible demonstrates uplifted regions centering on the fourth and twelfth alveoli.

Medially, the dentary's contribution to the mandibular symphysis is anteroposteriorly longer than it is tall. In dorsal view, it extends to the posterior margin of the fourth alveolus

(Fig. 13G) which is similar to *C. mylnarskii* but different from *B. formidabilis* which extends to alveoli 8–9. Similar to that of the *C. mylnarskii* holotype, sutural marks indicate an anterior splenial that is dorsoventrally short.

Although referred to *C. mylnarskii* by Estes (1988) the dissimilar toothrow morphology is the strongest evidence suggesting a separate species. Spacing of the anterior dentary alveoli differs between the specimens. Here, dentary alveoli 3–5 are closely spaced and alveoli 6–8 are widely spaced. The *C. mylnarskii* holotype preserves evenly spaced alveoli corresponding to positions 3–8. The largest posterior tooth is in the fourteenth position for YPM VPPU.017369 and the twelfth position for *C. mylnarskii*. The shape of the preserved teeth, when comparable to region or position indicate conical, blunt teeth for *C. mylnarskii* and pointed apices with varying degrees of buccolingual compression for YPM VPPU.017369. Morphology does not support YPM VPPU.017369 as a juvenile specimen of *C. mylnarskii* and comparison to *A. mississippiensis* for example indicates that apices become blunter over ontogeny but spacing of alveoli and degree of buccolingual compression do not change. In lateral view, both specimens preserve uplift of the posterior toothrow. This corresponds to the ninth alveolus and the region posterior to it in YPM VPPU.017369 (Fig. 13G) versus *C. mylnarskii* whose mandible demonstrates uplift centering on the twelfth alveolus (Fig. 13F). In both *C. mylnarskii* and this specimen, the dentary symphysis is anteroposteriorly longer than it is tall and extends to the posterior margin of the fourth alveolus (Fig. 13F, G). Similar to that of *C. mylnarskii*, sutural marks indicate an anterior splenial that is dorsoventrally short. Based on tooth proportions this specimen is a juvenile individual of a large

crocodyloid species and comparison to the larger YPM VPPU.018694 indicates an ontogenetic series.

YPM VPPU.018694

Estes (1988) records YPM VPPU.018694 as consisting of isolated teeth, vertebrae, and osteoderms. Today, only the teeth, collected by Princeton University in 1958 at the White Butte Site, remain associated with the lot and discussion with staff at YPM (APC personal communication with D. Brinkman, YPM, 2024) indicates that Estes (1988) may have confused these missing elements with another lot—subsequent searches did not locate the missing material.

Six tooth crowns of various sizes are associated with the lot. Comparison to tooth diversity and size in modern comparative specimens indicate that they may have belonged to a single individual but their position in the toothrow is unknown. All teeth preserve a strong, smooth mesiodistal carina and the largest crown measures 13 mm in mesiodistal diameter at its base and 30 mm from base to crown. The teeth are clearly similar to those of YPM VPPU.017369 based on proportions and morphology and suggest a large crocodyloid species at the site and an ontogenetic series with the smaller YPM VPPU.017369.

MATERIAL AND METHODS

Matrix

The matrix used in this analysis follows Cossette and Brochu (2020). Changes made to the matrix include the addition of *Chrysochampsa mylnarskii*, *Ahdeskatanka russlanddeutsche*, and updated character state coding for a number of alligatoroid species. The matrix contains 171 morphological characters and 111 ingroup taxa. Missing elements and obscured morphology limited the number of scorable characters for *Chrysochampsa mylnarskii* and *Ahdeskatanka russlanddeutsche*, which are scored for 41 and 47 of the 171 characters, respectively. See Supplementary File 2 for character/taxon matrix used in the phylogenetic analysis.

Methods

A maximum parsimony analysis was conducted to determine relationships among the ingroup taxa. Invariable characters among these taxa are excluded from this analysis and *Bernissartia fagesii* was used as an outgroup to root the trees. Matrices were managed in Mesquite v.3.81 (Maddison & Maddison, 2023). TNT v.1.5 (Goloboff et al., 2008) was employed to conduct a "New Technology" search utilizing all tree search methods (sectorial searches, ratchet, tree drifting, and tree fusing). For selections of size, the sectorial search parameters were set to 10 drifting cycles for both above and below the size of 75. For tree drifting, 10 rounds of the procedure were used. Minimum length trees were selected to be found 100 times. Collapsing rules and character weighting were not applied for the reconstructions. Multistate characters were treated as unordered.

Support of the nodes present in the most parsimonious trees was calculated using two different methods in TNT v.1.5 and values are presented in Figure S2A. The first method is bootstrapping, which resamples characters with replacement, infers pseudo-trees, and measures the support of every branch in the reference tree as the proportion of pseudo-trees containing that branch (Efron, 1979; Felsenstein, 1985). In this analysis 100,000 pseudoreplicates of the bootstrapping procedure were performed. GC frequencies summarize the topologies obtained during the bootstrap replicates and equal the percentage of trees supporting a given node minus the percentage of trees in conflict for a given node (Goloboff et al., 2003). The second

method is Bremer support, which evaluates nodes by exploring suboptimal trees to determine how many additional steps must be allowed in searching for tree topologies before a hypothesized clade is no longer recovered (Bremer, 1988, 1994).

Two tree methods summarize conflicting branching topologies in the most parsimonious trees. A strict consensus tree summarizes the most parsimonious trees recovered in the phylogenetic analyses and an Adams consensus tree improves resolution for labile taxa in the most parsimonious trees. The latter method preserves nesting information common to all most parsimonious trees and moves conflicting taxa to the lowest node common to those trees (Adams III, 1972). The strict consensus tree and Adams consensus tree were created in WinClada v.1.00.08 (Nixon, 2002) and PAUP* 4.0a169 (Swofford, 2002), respectively.

PHYLOGENETIC ANALYSIS

Results

Maximum parsimony analysis recovers 1385 shortest trees (see Supplemental File 3) (tree length = 664, consistency index with uninformative characters removed = 0.33, retention index = 0.83) and these trees are summarized in a strict consensus (Figs. 14A, S3). Some of the following clades are supported by homoplastic characters and the resulting optimizations are influenced by missing information as much as by preserved states.

In opposition to many published analyses using a similar dataset, which recover *Leidyosuchus canadensis* at the base of Alligatoroidea (Brochu, 2010, 2011; Cossette & Brochu, 2020; Hastings et al., 2016; Martin et al., 2014) here, the strict consensus tree recovers species of *Deinosuchus* as the basalmost alligatoroids. Crownward of the *Deinosuchus* clade the analysis recovers *Leidyosuchus canadensis*, Diplocynodontinae, Alligatoridae, and Alligatorinae + Caimaninae in a successive stepwise fashion. Alligatoroidea is defined on the basis of possessing no splenial process between the angular and coronoid, a foramen aerum that is inset from the margin of the retroarticular process, a maxilla that broadly separates the ectopterygoid from the maxillary toothrow, and a subequal to equal anterior process of the surangular.

In this analysis, crown alligatorids form two primary lineages—Alligatorinae and Caimaninae. Alligatorinae includes *Alligator mississippiensis* and all species of alligatoroids (its North American and Eurasian relatives) closer to it than to *Caiman crocodilus* and Caimaninae is defined by *Caiman crocodilus* and all species of alligatoroids (its North American and neotropical relatives) closer to it than to *Alligator mississippiensis*.

Chrysochampsa mylnarskii is recovered within Brachychampsini (Fig. 14), a stem-based clade phylogenetically defined as *Brachychampsa montana* and all alligatorids more closely related to it than to *Caiman crocodilus* or *Alligator mississippiensis*. This group of North American species, hitherto known only from the Upper Cretaceous, is recovered at the base of Caimaninae in common to analyses performed by one of the authors (Cossette & Brochu, 2018; Cossette, 2021) and results in the stem-based Globidonta of Brochu (1999) —*Alligator mississippiensis* and all alligatoroids closer to it than to *Diplocynodon ratelii*—as synonymous with Alligatoridae.

Within Brachychampsini, *C. mylnarskii* is sister to species of *Brachychampsa*, *Stangerochampsa mccabei* and *Albertochampsa langstoni* form a polytomy with the clade (Fig. 14). Brachychampsini is diagnosed on the character basis of a uniformly narrow scapulocoracoid facet anterior to the glenoid fossa, a large incisive foramen that intersects the premaxillary–maxillary suture, long dorsal premaxillary processes extending beyond the third maxillary alveolus, and a frontoparietal suture that makes modest entry into supratemporal fenestra at maturity and whose postorbital and parietal are in broad contact. The first of
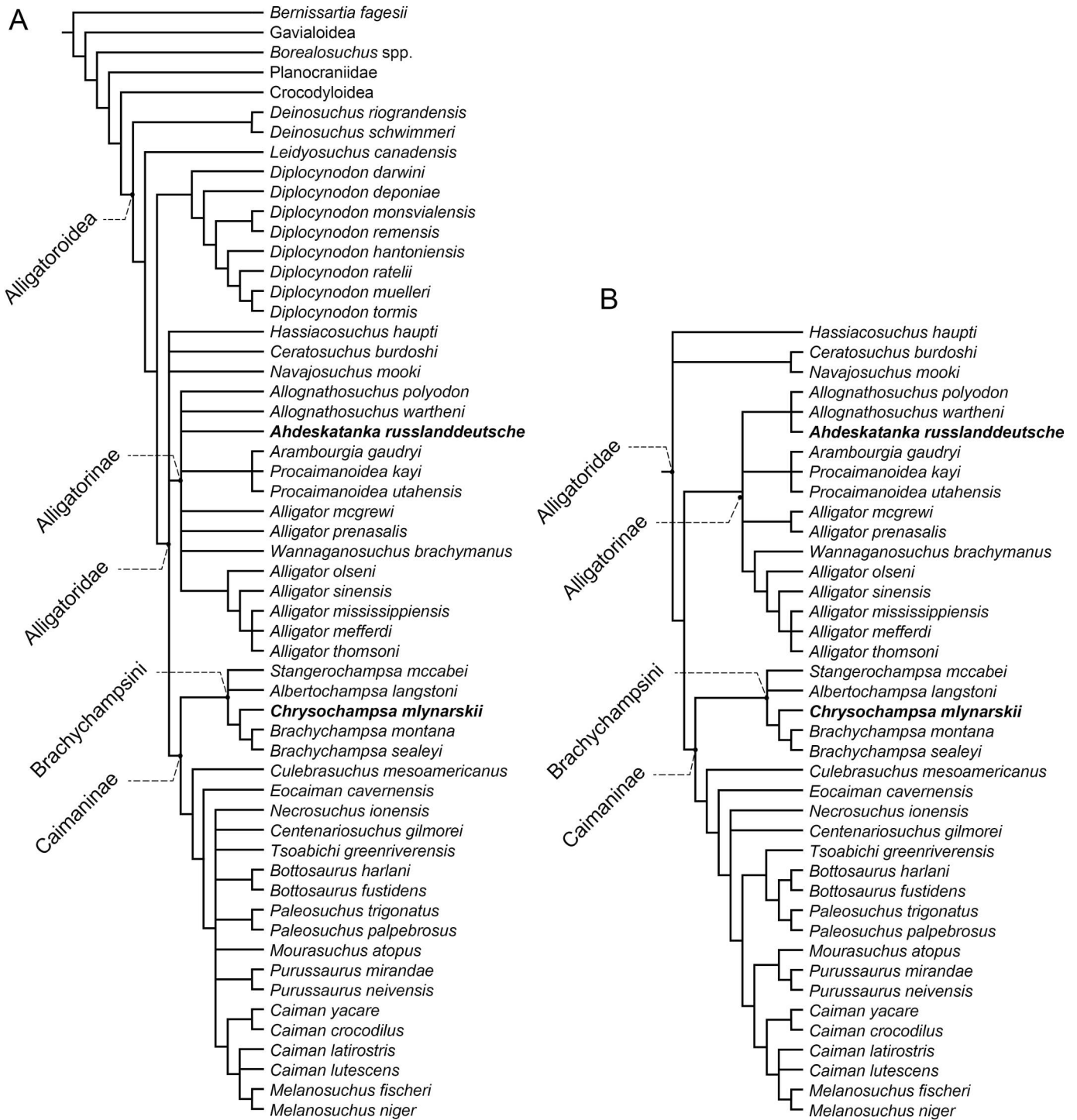
FIGURE 14. Consensus trees showing the placement of *Ahdeskatanka russlanddeutsche*, YPM VPPU.016990 holotype specimen and *Chrysochampsa mylnarskii*, YPM VPPU.017258 holotype specimen within Alligatoridae. **A**, strict consensus tree: total trees = 1385, tree length = 664, consistency index = 0.33, retention index = 0.83. **B**, Adams consensus tree of Alligatoridae.

these is the basal state for Crocodylia in this analysis with the Diplocynodontinae + Alligatoridae group possessing the derived state and two additional reversals in the clade including *C. mylnarskii* and another in the *Mourasuchus atopus* + species of *Purussaurus* clade.

Chrysochampsa mylnarskii is diagnosed in the phylogenetic analysis by a dentary symphysis that extends to the fourth alveolus and a splenial that is excluded from the mandibular symphysis and whose anterior tip passes dorsal to the Meckelian groove. Character support for a sister group relationship with the two species of *Brachychampsa* is via possession of a mandibular ramus of CN V that exits the anterior splenial only and large exposures of the supraoccipital on the dorsal surface of the skull table. The first character state is plesiomorphic at the level of

Alligatoroidea with derived states evolving in species of *Diplocynodon*, *A. mississippiensis*, *C. mylnarskii* + species of *Brachychampsa*, and derived caimanines. The second is derived independently within Caimaninae in the *C. mylnarskii* + *Brachychampsa* clade, *Tsoabichi* + *Bottosaurus* + *Paleosuchus* clade, and again in species of *Purussaurus*.

The topology of Alligatorinae is stable with the exception of a few labile species, including *A. russlanddeutsche* and its closest relatives in the analyses presented here. The lability of these taxa is not new to this analysis (Brochu, 2004) and species of *Allognathosuchus* have proven difficult to distinguish from other Paleogene alligatorids. An Adams consensus tree provides additional resolution and recovers the new species in a clade with species of *Allognathosuchus* (Fig. 14B).

Ahdeskatanka russlanddeutsche is diagnosed by a large incisive foramen that intersects the premaxillary–maxillary suture, long dorsal premaxillary processes that extend beyond the third maxillary alveolus, and a linear frontoparietal suture. Depending on within-group topology, the *A. russlanddeutsche* + *A. polyodon* + *A. wartheni* clade is diagnosed by either a straight pterygoid ramus of the ectopterygoid and a linear posterolateral margin of the suborbital fenestra or a surangular–dentary suture that intersects the posterodorsal corner of the external mandibular fenestra. Among the most parsimonious trees, most recover these taxa in a clade that also includes species of *Procaimanoidea* and *Arambourgia gaudryi*, but that clade's diagnosis also depends on within-group topology (Fig. S2B).

SPECIES IDENTITY AND NUMBER AT THE SOUTH HEART LOCALITY

The incompleteness of the fossil record hinders determination of species diversity at all scales, and the South Heart Locality is no different. Whereas nearly complete cranial material is known for *A. russlanddeutsche* and *C. mylnarskii*, other species are known from few elements. Here, a discussion of elements providing the greatest efficacy to provide a minimum number of species at the South Heart Locality is undertaken.

Dentaries

The locality does not preserve any complete mandibles but dentaries are the best available elements to determine the number of species present (Fig. 13). These elements, belonging to numerous individuals, reveal a diverse contemporaneous crocodylian fauna occupying multiple niches. *Chrysochampsa mylnarskii* preserves a blunt, U-shaped mandible with generalized, conical, low crowned dentition. A presumed crocodyloid, YPM VPPU.017369, is represented by a V-shaped mandible with high crowned dentition and acute apices. Specimens referable to *A. russlanddeutsche* and YPM VPPU.030625 represent two, small, closely related yet morphologically distinct taxa preserving blunt crowned dentition characterized by a distal series of enlarged teeth. Although assignment to species level is not feasible for all specimens these dentaries are consistently differentiated, represent eight individuals, and belong to at least four species. Assignment at higher taxonomic levels indicates three alligatorids and one crocodyloid.

Dentaries tentatively assigned to *A. russlanddeutsche* (YPM VPPU.016902, YPM VPPU.016996, YPM VPPU.030621) (Figs. 11, 13) preserve strikingly similar suites of character states including: a broad, U-shaped mandible; a pronounced dorsal uplift along the posterior toothrow beginning at the tenth alveolus; broad curvature of the toothrow between alveoli four and 10; diagnostic proportions of alveolar margins and spacing of anterior alveoli; the largest alveolus in the posterior arcade is in the thirteenth position; preserved teeth are conical and low crowned, or blunt and globular; a dentary symphysis extending

to the seventh or eighth alveolus; and a pronounced ridge separating dorsal from lingual surfaces of the medial dentary.

Morphology differentiates these dentaries from *C. mylnarskii*, YPM VPPU.030625, and YPM VPPU.017369 by proportions and spacing of alveoli, dentary symphysis length, and dorsal uplift of the toothrow (Fig. 13). Comparison to species of *Allognathosuchus*, recovered alongside *A. russlanddeutsche* in phylogenetic analyses presented here, suggests that these dentaries preserve common morphological features shared by the more inclusive taxonomic group. Although the *A. russlanddeutsche* holotype (Fig. 3) does not preserve a complete dentary, morphologies of close relatives, and separation of the phylogenetically allied species in time and space suggests a tentative referral of the specimens here to *A. russlanddeutsche*.

Comparison to *Allognathosuchus*, the phylogenetically allied *Arambourgia gaudryi*, and species of *Procaimanoidea* reveals disparity and similarity in mandibular character states. Specimens referred to *A. russlanddeutsche* (YPM VPPU.016996, YPM VPPU.016902, YPM VPPU.030621) (Figs. 11, 13) preserve dentary symphyses exceeding the length found in species of *Procaimanoidea* and *A. gaudryi* but similar to species of *Allognathosuchus*. Shared between all closely allied species considered in this discussion, YPM VPPU.016996, YPM VPPU.016902, and YPM VPPU.030621 preserve deeply curved dentary toothrows between alveoli four and 10. Common to species of *Allognathosuchus*, both YPM VPPU.016996 and YPM VPPU.016902 preserve dentaries whose largest alveolus is in the thirteenth position with a series of large teeth distal to it—preservation of the region is incomplete in YPM VPPU.030621. Contrary to this morphology, species of *Procaimanoidea* and *A. gaudryi* preserve the largest dentary alveolus in the same region, but without the distal series of large alveoli. Additional morphological differentiation is possible using character states not included in the phylogenetic analysis. The region of dorsal uplift along the posterior toothrow begins at the tenth dentary alveolus in YPM VPPU.016996, YPM VPPU.016902, and species of *Allognathosuchus*, but differs from species of *Procaimanoidea* and *A. gaudryi* whose uplift is more gradual and not as tall in lateral view.

YPM VPPU.030625 (Figs. 12G, 13D) is a blunt, U-shaped mandible with a single low crowned tooth. This element represents a small-bodied alligatorid taxon and is differentiated from *C. mylnarskii* and YPM VPPU.017369 via the length of the dentary symphysis, dorsal uplift of the posterior toothrow, and curvature of the mid-dentary toothrow between alveoli four and 10. Referral to *A. russlanddeutsche* is also unlikely as the dentary symphysis is shorter, the posterior dorsal uplift of the toothrow is positioned more anteriorly, the anterior alveoli are evenly spaced, and the curvature of the toothrow between alveoli four and 10 is less pronounced. Yet dental morphology and the robust proportions of the gross specimen suggest a somewhat close relationship to the new species and indicate another small-bodied alligatorid within the formation.

Here, in disagreement with Estes (1988), the authors do not assign additional YPM VPPU specimens to *C. mylnarskii*. Nevertheless, the holotype dentary (Fig. 3) for that species preserves a suite of character states differentiating it from all other mandibles at the locality. These include the following: a broad, U-shaped mandible; a dentary symphysis that extends to the fourth alveolus; a dorsal uplift along the distal toothrow which centers on the twelfth alveolus; a straight toothrow between alveoli four and 10; unique proportions of alveolar margins and spacing of alveoli; preserved teeth are conical and low crowned or blunt; the twelfth position is the largest alveolus in the distal arcade.

The *C. mylnarskii* holotype redescribed here preserves morphology contrasting with that of all known specimens from the locality (Fig. 13). Phylogenetic analyses presented here recover *C. mylnarskii* as sister to species of *Brachychampsa* and

immediately crownward of *Stangerochampsa mccabei* and *Albertochampsa langstoni*. Here, the mandible of *C. mylnarskii* is differentiated from these taxa by a shorter dentary symphysis, the largest distal alveolus is in the twelfth dentary position, and a splenial that is excluded from the mandibular symphysis and whose anterior tip passes dorsal to the Meckelian groove.

YPM VPPU.017369 (Figs. 12J, 13G) tentatively represents a crocodyloid with a V-shaped mandible, high crowned dentition, strong mesiodistal carinae, and acute apices. These features are unlike all other mandibles preserved at the locality, but shared with species of *Borealosuchus*, though differentiated by a much shorter dentary symphysis and the lack of confluent third and fourth dentary alveoli in YPM VPPU.017369.

Frontals

Four frontals are known from the South Heart Locality. In addition to frontals preserved by *C. mylnarskii* and *A. russlanddeutsche* holotype specimens (Figs. 3, 6) two elements are known for YPM VPPU.030624 (Fig. 12B), which is not referable to species. All frontals preserve indentations of the dorsal surface and pronounced sculpturing but the latter differs between the species. Frontals from YPM VPPU.030624 and *C. mylnarskii* preserve sculpturing of similar depth whose ornamentation is mostly circular and evenly spaced. In contrast, sculpturing is deep and ovoid, with irregular spacing in *A. russlanddeutsche.*

Measurements taken at the point of greatest mediolateral constriction between the orbits divided by the widest part of the posterior frontal, reveals three divergent proportions. *Chrysochampsa mylnarskii* has the lowest proportion (0.29), *A. russlanddeutsche* the highest (0.66), and YPM VPPU.030624 is intermediate to them (0.44 and 0.45).

Sutural shapes differentiate the species. Although incompletely known for *C. mylnarskii*, the sutural contact with the prefrontals differs among *A. russlanddeutsche*, whose suture is convex, and YPM VPPU.030624, which preserves a linear suture. The directionality of the sutural contact with the postorbital is roughly mediolaterally oriented in *C. mylnarskii*, anteroposteriorly linear in *A. russlanddeutsche*, and laterally trending from anterior to posterior in YPM VPPU.030624. The sutural contact with the parietal is posteriorly convex in both *C. mylnarskii* and YPM VPPU.030624, but linear in *A. russlanddeutsche*. The anterior W-shaped sutural contact with the nasals is similar among the species.

The frontals preserved by YPM VPPU.030624, only slightly smaller than that of the *A. russlanddeutsche* holotype, preserve few similarities with the types. Proportions of the element and shape of sutural contacts are demonstrably divergent among the species.

Teeth

The locality preserves both socketed and loose teeth. *Chrysochampsa mylnarskii* (Fig. 3) preserves conical teeth with blunt apices whose distalmost dentition bears moderate buccolingual compression; *A. russlanddeutsche* (Fig. 6) and specimens assigned to it (Fig. 11) preserve small, low crowned, conical or blunt dentition; and YPM VPPU.017369 (Fig. 12J) preserves dentition with distinct apices and buccolingual compression throughout the arcade. YPM VPPU.018694 preserves teeth of various sizes that are invariably long and pointed, similar to YPM VPPU.017369, and indicates a large crocodyloid or a species of *Borealosuchus* was present at the locality.

Osteoderms

The locality preserves osteoderms representing three morphotypes from an unknown number of individuals. *Chrysochampsa mylnarskii* preserves square, unkeeled dorsal osteoderms (Fig. 5B). A small, keeled osteoderm (Fig. 12A) known from the locality may represent *A. russlanddeutsche*. A single, rectangular osteoderm (Fig. 12A) preserves a mediolaterally long axis and a small but poorly preserved part of an anterolateral process as found in species of *Borealosuchus* (Brochu et al., 2012).

ECOLOGY OF LOCALITY

Today, there are few examples of different species of crocodylians coexisting (Shirley et al., 2014). These regions often include one wide-ranging species overlapping with a species whose range is restricted (Shaney et al., 2017; Shirley et al., 2015; Staniewicz et al., 2018). This range overlap does not mean the species are syntopic and many sympatric crocodylian species occupy different habitats within a given catchment (Ouboter, 1996). Among the crocodylians at the South Heart Locality, we cannot comment on the occupation of different habitats, but rather the existence of these specimens in the same time and place. Regardless, the presence of so many species in close proximity differs from the modern record and is notable even among fossil localities.

Among the Golden Valley crocodylian fauna, niche partitioning is clearly evidenced by differences in size, snout shape, and dentition. *Chrysochampsa mylnarskii* has a long, broad snout and conical teeth similar to *A. mississippiensis*, a taxon regarded as an ecological generalist capable of eating anything it can swallow (Dodson, 1975; Ouchley, 2013; Saalfeld et al., 2011). YPM VPPU.017369 and YPM VPPU.018694 represent large generalists similar to species of modern *Crocodylus* with a V-shaped mandible and dentition with large, pointed apices, respectively. *Ahdeskatanka russlanddeutsche*, YPM VPPU.030625, and most Paleogene alligatorids share short snouts with large, blunt distal teeth. Historically, the robust mandibular rami, long dentary symphyses, and tooth proportions provided evidence for a specialized durophagous diet (Abel, 1928; Carpenter & Lindsay, 1980; Case, 1925) and Aoki (1989) hypothesized that the elevated jaw joints allowed for grinding motions along the distal toothrow in these taxa. It is unknown if these brevirostrine crocodylians were ecological specialists or generalists (Bartels, 1984; Brochu, 2004; Simpson, 1930), and debate surrounding the functional significance of their morphology continues. Yet, the craniodental morphology of these small alligatorid taxa suggests a different feeding strategy from *C. mylnarskii* and YPM VPPU.017369.

Morphological disparity evident among the locality's crocodylians indicates a complex food web with adults of the smaller species acting as mesopredators, and the larger species acting as apex predators. Additional niche partitioning happens over the span of ontogeny with post-hatchlings, juveniles, and adults of the same species competing for different resources. Results from the majority of studies suggest that all crocodylians are opportunistic predators consuming invertebrates and small vertebrates as juveniles with larger adult body sizes corresponding to consumption of larger prey (Borteiro et al., 2009; Delany & Abercrombie, 1986; Platt et al., 2006; Saalfeld et al., 2011). This behavior is widespread among taxa separated by tens of millions of years of phylogenetic history, and we assume that these trends existed in the fossil record and complicated both inter- and intraspecies niche partitioning at the South Heart Locality.

Alligatorids represent the majority of large predatory niches within the locality and all taxa recovered here preserve variously blunt snouts and conical or globular teeth. These taxa, represented by two small-bodied species and one larger species, show limited phylogenetic and morphological diversity. The nature of their interspecific niche partitioning is unknown, but modern small-bodied crocodylians are relatively more terrestrial than larger species and are known to venture into forested areas

near wetlands (Eaton, 2010; Magnusson & Campos, 2010). The greater ease in which a small-bodied species locomotes through complex forested terranes would also apply to their fossil relatives, and may provide additional niche partitioning and a reduction in competition among these co-occurring taxa.

The South Heart Locality has yielded a highly diverse crocodylian fauna, but has a conspicuous lack of large-bodied mammalian carnivore taxa noted by previous workers (Jepsen, 1963). "Creodonts" were particularly diverse during the early Eocene (Wasatchian), but larger examples, including any representatives of Oxyaenidae or Mesonychidae, are absent from the White Butte assemblage, and Hyaenodonts are represented by a single M2 tooth with root (YPM VPPU.017337) tentatively assigned to the genus *Sinopa* (Jepsen, 1963; West, 1973). Carnivoran genera *Miacis* and *Didymictis* have also been collected from the South Heart Locality but are relatively small-bodied.

The fossil-bearing horizon at the White Butte and Turtle Valley sites is found amidst carbonaceous shales in the interchannel facies of the Camels Butte Member (Fig. 2) (Hickey, 1967; Jepsen, 1963). The low energy environment represented by the locality, as well as its stratigraphic proximity to the silicified lignite hard siliceous layer (Fig. 2), are suggestive of a swamp-like environment (Hickey, 1967). This paleoenvironmental reconstruction may explain both the lack of large-bodied mammalian predators as well as the high diversity of crocodylians. A waterlogged setting like this could put crocodylian taxa at a competitive advantage for any tetrapod prey, effectively excluding the larger mammalian species that would otherwise inhabit the region (Jepsen, 1963).

Modern environments characterized by swamps and dense forests, similar to the paleoenvironmental reconstruction of the South Heart Locality, are noted for supporting fewer large-bodied mammalian carnivoran species compared with other habitats (Bogoni et al., 2018; Mendoza et al., 2005). Large predatory niches in these environments are instead often occupied by reptiles (Magnusson & Lima, 1991), and when present in the ecosystem larger mammalian predators are typically rare (Brown et al., 2006; Sasidhran et al., 2016). Being semiaquatic ambush predators (Nagloo et al., 2016; Somaweera et al., 2020), crocodylians may possess a competitive advantage in areas with large bodies of stagnant water and swamps and swamp forests are the preferred habitats for some extant crocodylian species (Stuebing et al., 2006). Mammalian predators are also reported as being reluctant to cross reaches of swampy water (Frederick & Collopy, 1989) and this would limit their ability to traverse any such habitat. The relatively low metabolic requirements of crocodylians relative to mammals may also play an important role in affecting the observed differences in relative abundance (Magnusson & Lima, 1991) at the South Heart Locality.

DISCUSSION

The most conspicuous aspect of the crocodylian fauna at the South Heart Locality is its lack of phylogenetic diversity. *Ahdeskatanka russlanddeutsche* preserves many character states common to a suite of distantly related North American Paleogene alligatorids, resulting in conflicting most parsimonious trees and reduced resolution. In the Adams consensus presented as part of this study (Fig. 14B), *A. russlanddeutsche* is recovered in a polytomy with species of Eocene age *Allognathosuchus*. Character and nodal support metrics (Fig. S2A) provide robust phylogenetic hypotheses suggesting that *Chrysochampsa mylnarskii* is a late surviving member of Brachychampsini, an alligatorid group hitherto known from the Late Cretaceous.

Previous work by Lucas and Sullivan (2004) revisited the *C. mylnarskii* holotype and determined it to be a junior subjective synonym of the geographically widespread, and taxonomically complicated (Brochu, 2004) Paleogene alligatorid genus *Allognathosuchus*. Their referral was based on disagreement with the diagnosis of Estes (1988), and used general similarities based on snout width, dentition, toothrow, and characteristics of the splenial. In agreement with the analysis here, Brochu (2004) noted that the general similarities of Lucas and Sullivan (2004) apply to all basally branching alligatorines, and *C. mylnarskii* does not have an extensive contribution of the splenial to the mandibular symphysis. In this work, Brochu (2004) distinguished *C. mylnarskii* from all Paleogene alligatoroids, but suggested that its relationships to other members of the clade were unclear. However, these authors did not conduct phylogenetic analyses to reach their taxonomic conclusions.

In agreement with Estes (1988), the phylogenetic hypotheses produced as part of this project indicate *C. mylnarskii* to be an alligatorid crocodylian. The *C. mylnarskii* holotype unmistakably represents a separate species, and is distinguished by a suite of characters from members of its relict Cretaceous clade, species of *Allognathosuchus*, and alligatoroids from the same approximate time. Here, the authors extend the diagnosis of Estes (1988) to a suite of unique and shared character states of the frontal bone, external nasal aperture, dentary symphysis, dentary teeth, atlas intercentrum, and dorsal osteoderms. Unique among contemporaneous alligatorids, the width of the posterior frontal in *C. mylnarskii* is so great that it excludes the postorbitals from contacting the posterior orbital margin. As opposed to Upper Cretaceous and Paleogene alligatorids, whose nasals extend into the external nasal aperture as distinct points, the nasals of *C. mylnarskii* end in blunt points forming the posterior margin of the aperture. Unlike species of *Allognathosuchus*, the closely allied *Stangerochampsa mccabei*, and species of *Brachychampsa* whose dentary symphyses extend to the sixth through eighth dentary alveoli, *C. mylnarskii* preserves a symphysis that extends to the fourth alveolus. The contribution of the splenial in the mandibular symphysis is robust in Paleogene alligatorids, but is extremely slight and passes dorsal to the Meckelian groove in *C. mylnarskii*.

The distal teeth of *C. mylnarskii* differ from those of its closest relatives. Unlike *A. langstoni*, *S. mccabei*, and species of *Brachychampsa*, which preserve globular distalmost upper and lower dentition, the corresponding teeth of *C. mylnarskii* are similar to the teeth of a generalist alligatorid such as *A. mississippiensis*. The combination of a shorter dentary symphysis, lack of robust contribution of the splenial in the mandibular symphysis, and generalist teeth suggest a dietary shift in *C. mylnarskii* driven by competition with the more efficient crushing morphology of the small-bodied, globular toothed alligatorids at the South Heart Locality.

Support for *A. russlanddeutsche* in the phylogenetic analyses presented here (Fig. S2A) is weaker than that of *C. mylnarskii* but is differentiated from all Paleogene alligatorid species by morphology not included in the matrix. *Ahdeskatanka russlanddeutsche* is recovered alongside the small-bodied Eocene species of *Allognathosuchus* included in this study (Fig. 14B). The generic name *Allognathosuchus* was originally applied by Mook (1921) to fossil crocodylians from the Eocene age Bridger Formation of Wyoming but has been applied to Upper Cretaceous through Oligocene fossils from North America, South America, Europe, Asia, and Africa. Various authors have referred 15 species in various states of completeness and preservation to the genus, and references to *Allognathosuchus* in the literature often rely on isolated, bulbous teeth. The teeth, originally regarded as diagnostic (Mook, 1921) are found in several crocodyliform lineages and are not distinguishable to the level of genus (Hutchinson & Kues, 1985) complicating the use of *Allognathosuchus* as a dental form taxon.

The complex systematic history of the genus *Allognathosuchus* and the lack of resolution in the strict consensus tree complicates

efforts. Although the Adams consensus tree recovers *A. russlanddeutsche* in a clade with species of *Allognathosuchus*, in agreement with Brochu (2004) the phylogenetic results here suggest that the name *Allognathosuchus* should be restricted to *A. polyodon* and *A. wartheni*. Considering the dissonance between the trees, and the relatively weak character support for the clade, the authors cannot provide definitive evidence for the membership of the new taxon in *Allognathosuchus*. Here, a new genus erected based on morphologically distinct fossils solves these issues.

Previous non-cladistic work recovered the blunt toothed, short-snouted fossil taxa together sharing a common ancestor with modern alligatorids (Case, 1925; Kälin, 1936; Mook, 1941; Simpson, 1930). Recent cladistic analyses do not support this grouping, and some analyses recover subsets of these specialized species as more closely related to species of modern *Alligator* than to other blunt-snouted fossil species (Brochu, 2004; Wu et al., 1996). Some modern analyses recover *Alligator* as not monophyletic, and fossil species of the genus with snouts strikingly similar to that of modern *Alligator* are nested within clades including the short-snouted species discussed here (Brochu, 1999, 2004; Cossette, 2021; Williamson, 1996: Wu et al., 1996). The cranial anatomy thought to diagnose species of *Allognathosuchus*, and both closely and distantly related Paleogene forms, is plesiomorphic at the level of Alligatoridae.

CONCLUSION

The lower Eocene South Heart Locality within the Golden Valley Formation of Stark County, North Dakota reveals a speciose, sympatric crocodylian fauna during one of the hottest sustained intervals in Earth history. These species inhabited a warm and humid environment dominated by swamps and marshes with dense subtropical forests along sinuous rivers and streams. These diverse crocodylians existed alongside richly preserved riparian and aquatic taxa allowing for paleoecological reconstructions and an exploration of their niche partitioning. The locality's trophic dynamics diverge from modern environments and the various crocodylian taxa may have filled the ecological niche of large mammalian carnivores conspicuously absent here.

The South Heart Locality crocodylians provide extensive morphological data during the Paleogene North American alligatorid diversity peak. Coeval with this peak, most species recovered from the locality are alligatorids, and reveal a notably limited level of phylogenetic diversity for the crocodylian community.

The Golden Valley Formation crocodylian species are consistently differentiated and represent a minimum of four morphotypes partitioned by size, bauplan, and inferred feeding strategy. The possible presence of a fifth crocodylian species is suggested by limited dental and osteoderm evidence. Shared with many alligatorid species from the Upper Cretaceous and Paleogene of North America, the locality's small-bodied taxa preserve globular distal teeth, blunt snouts, massive jaws, and long dentary symphyses indicative of durophagous predators.

A new genus and species is described and a previously known holotype is redescribed. The phylogenetic relationships of *A. russlanddeutsche* and *C. mylnarskii* reveal an additional data point documenting the explosive radiation of small-bodied alligatorids in the Paleogene of North America, and a range extension for a clade previously known from the Cretaceous, respectively. The small-bodied *Ahdeskatanka russlanddeutsche* preserves the ancestral alligatorid feeding strategy with globular distal dentition and a blunt snout. It is an exemplar of a radiation of small-bodied alligatorids with crushing dentition and preserves the ancestral alligatorid feeding strategy. The second

species, *Chrysochampsa mylnarskii*, is recovered as sister to species of *Brachychampsa* and nested within Brachychampsini. Character support for this topology is strong but the taxon lacks some features shared by other members of the clade. The feeding apparatus of the species diverges in its functional morphology from closest relatives and likely represents a shift in feeding strategy to minimize competition with the crushing adapted species coexisting in the region.

This manuscript, describing the crocodylian taxa of the Golden Valley Formation at two closely spaced sites within a single locality and interval, is one part of a larger project. Prior to this work, efforts to describe crocodylian specimens from the locality had been limited. Here, trophic dynamics at the locality are elucidated and phylogenetic relationships determined for the endemic, highly diverse crocodylian community. Lush, highly productive ecosystems preserved at the South Heart Locality sites inform the evolutionary history of North American alligatorids and preserve significant biodiversity following the Paleocene–Eocene Thermal Maximum.

DATA AVAILABILITY STATEMENT

The authors confirm that the data supporting the findings of this study are available within the article and the linked supplementary materials.

AUTHOR CONTRIBUTIONS

APC designed the project, gathered the data, analyzed the data, and drafted the majority of the manuscript. DAT analyzed the data, and drafted sections of the manuscript. All authors edited the manuscript.

SUPPLEMENTARY FILES

Supplementary File 1.docx: Supplementary Figures S1–S3.
Supplementary File 2.nex: Combined morphological matrix and character list used in the phylogenetic analysis.
Supplementary File 3.zip: Most parsimonious trees recovered from the phylogenetic analysis.

ORCID

Adam P. Cossette http://orcid.org/0000-0002-8030-0112

LITERATURE CITED

Abel, O. (1928). *Allognathosuchus*, ein an die cheloniphage Nahrungsweise angepasster Krokodiltypus des nordamerikanischen Eozäns. *Paläontologische Zeitschrift*, 9(4), 367–374. doi:10.1007/BF03041562

Adams III E. N. (1972). Consensus techniques and the comparison of taxonomic trees. *Systematic Biology*, 21(4), 390–397. doi:10.1093/sysbio/21.4.390

Aoki, R. (1989). The jaw mechanics in the heterodont crocodilians. *Current Herpetology in East Asia*, 1, 17–21.

Bartels, W. (1984). Osteology and systematic affinities of the horned alligator *Ceratosuchus* (Reptilia, Crocodilia). *Journal of Paleontology*, 58, 1347–1353.

Benson, W. E. (1949). Golden Valley Formation of North Dakota [Abstract]. *Geological Society of America Bulletin*, 60, 1873–1874.

Benson, W. E. (1953). Geology of the Knife River area, North Dakota. *U.S. Geological Survey Open File Report*, 53–21.

Benson, W. E., & Laird, W. M. (1947). Eocene of North Dakota: abstract. *Geological Society of America Bulletin*, 58(12), 1166–1167.

Benton, M. J., & Clark, J. M. (1988). *Archosaur phylogeny and the relationships of the Crocodylia*. In M. J. Benton (Ed.), *The Phylogeny and Classification of the Tetrapods* (pp. 295–338). Clarendon Press.

Bogoni, J. A., Pires, J. S. R., Graipel, M. E., Peroni, N., & Peres, C. A. (2018). Wish you were here: How defaunated is the Atlantic Forest biome of its medium–to large–bodied mammal fauna? *PloS one*, 13(9), e0204515. doi:10.1371/journal.pone.0204515

Borteiro, C., Gutiérrez, F., Tedros, M., & Kolenc, F. (2009). Food habits of the Broad–snouted Caiman (*Caiman latirostris*: Crocodylia. *Studies on Neotropical Fauna and Environment*, 44(1), 31–36. doi:10.1080/01650520802507572

Bremer, K. (1988). The limits of amino acid sequence data in angiosperm phylogenetic reconstruction. *Evolution*, 42(4), 795–803. doi:10.2307/2408870

Bremer, K. (1994). Branch support and tree stability. *Cladistics*, 10(3), 295–304. doi:10.1111/j.1096-0031.1994.tb00179.x

Brochu, C. A. (1999). Phylogenetics, taxonomy, and historical biogeography of Alligatoroidea. *Journal of Vertebrate Paleontology*, 19(S2), 9–100. doi:10.1080/02724634.1999.10011201

Brochu, C. A. (2001). Crocodylian snouts in space and time: phylogenetic approaches toward adaptive radiation. *American Zoologist*, 41(3), 564–585.

Brochu, C. A. (2003). Phylogenetic approaches toward crocodylian history. *Annual Review of Earth and Planetary Sciences*, 31(1), 357–397. doi:10.1146/annurev.earth.31.100901.141308

Brochu, C. A. (2004). Alligatorine phylogeny and the status of *Allognathosuchus* Mook, 1921. *Journal of Vertebrate Paleontology*, 24(4), 857–873. doi:10.1671/0272-4634(2004)024[0857:APATSO]2.0.CO;2

Brochu, C. A. (2010). A new alligatorid from the Lower Eocene Green River Formation of Wyoming and the origin of caimans. *Journal of Vertebrate Paleontology*, 30(4), 1109–1126. doi:10.1080/02724634.2010.483569

Brochu, C. A. (2011). Phylogenetic relationships of *Necrosuchus ionensis* Simpson, 1937 and the early history of caimanines. *Zoological Journal of the Linnean Society*, 163(s1), S228–S256. doi:10.1111/j.1096-3642.2011.00716.x

Brochu, C. A., Parris, D. C., Grandstaff, B. S., DentonJrR. K., & Gallagher, W. B. (2012). A new species of *Borealosuchus* (Crocodyliformes, Eusuchia) from the Late Cretaceous–early Paleogene of New Jersey. *Journal of Vertebrate Paleontology*, 32(1), 105–116. doi:10.1080/02724634.2012.633585

Brown, M. T., Cohen, M. J., Bardi, E., & Ingwersen, W. W. (2006). Species diversity in the Florida Everglades, USA: A systems approach to calculating biodiversity. *Aquatic Sciences*, 68(3), 254–277. doi:10.1007/s00027-006-0854-1

Carpenter, K., & Lindsey, D. (1980). The dentary of *Brachychampsa montana* Gilmore (Alligatorinae; Crocodylidae), a Late Cretaceous turtle–eating alligator. *Journal of Paleontology*, 54, 1213–1217.

Case, E. C. (1925). Note on a new species of the Eocene crocodilian *Allognathosuchus*, *A. wartheni*. *Contributions from the Museum of Geology, University of Michigan*, 2, 93–97.

Clarac, F., Souter, T., Cornette, R., Cubo, J., & de Buffrenil, V. (2015). A quantitative assessment of bone area increase due to ornamentation in the Crocodylia. *Journal of Morphology*, 276(10), 1183–1192. doi:10.1002/jmor.20408

Clechenko, E. R., Kelly, D. C., Harrington, G. J., & Stiles, C. A. (2007). Terrestrial records of a regional weathering profile at the Paleocene–Eocene boundary in the Williston Basin of North Dakota. *Geological Society of America Bulletin*, 119(3–4), 428–442. doi:10.1130/B26010.1

Cossette, A. P. (2021). A new species of *Bottosaurus* (Alligatoroidea: Caimaninae) from the Black Peaks Formation (Palaeocene) of Texas indicates an early radiation of North American caimanines. *Zoological Journal of the Linnean Society*, 191(1), 276–301. doi:10.1093/zoolinnean/zlz178

Cossette, A. P., & Brochu, C. A. (2018). A new specimen of the alligatoroid *Bottosaurus harlani* and the early history of character evolution in alligatorids. *Journal of Vertebrate Paleontology*, 38(4), 1–22. doi:10.1080/02724634.2018.1486321

Cossette, A. P., & Brochu, C. A. (2020). A systematic review of the giant alligatoroid *Deinosuchus* from the Campanian of North America and its implications for the relationships at the root of Crocodylia. *Journal of Vertebrate Paleontology*, 40(1), e1767638. doi:10.1080/02724634.2020.1767638

Cozzuol, M. A. (2006). The Acre vertebrate fauna: age, diversity, and geography. *Journal of South American Earth Sciences*, 21(3), 185–203. doi:10.1016/j.jsames.2006.03.005

Cuvier, G. L. (1807). Sur les differentes especes de crocodiles vivan set sur leur caracteres distinctifs. *Annales du Museum d'Histoire Naturelle*, 10, 8–66.

Daudin, F. M. (1802). *Histoire Naturelle, Générale et Particulière des Reptiles; Ouvrage faisant suite à l'Histoire Naturelle générale et particulière, composée par Leclerc de Buffon; et rédigée par C.S. Sonnini, membre de plusieurs sociétés savants (Vol. 2)*. F. Dufart.

de Buffrénil, V. (1982). Morphogenesis of bone ornamentation in extant and extinct crocodilians. *Zoomorphology*, 99(2), 155–166. doi:10.1007/BF00310307

de Buffrénil, V., Clarac, F., Fau, M., Martin, S., Martin, B., Pellé, E., & Laurin, M. (2015). Differentiation and growth of bone ornamentation in vertebrates: a comparative histological study among the Crocodylomorpha. *Journal of Morphology*, 276(4), 425–445. doi:10.1002/jmor.20351

De Celis, A., Narváez, I., & Ortega, F. (2020). Spatiotemporal palaeodiversity patterns of modern crocodiles (Crocodyliformes: Eusuchia). *Zoological Journal of the Linnean Society*, 189(2), 635–656. doi:10.1093/zoolinnean/zlz038

Delany, M. F., & Abercrombie, C. L. (1986). American alligator food habits in northcentral Florida. *The Journal of Wildlife Management*, 50(2), 348–353. doi:10.2307/3801926

Dodson, P. (1975). Functional and ecological significance of relative growth in *Alligator*. *Journal of Zoology*, 175(3), 315–355. doi:10.1111/j.1469-7998.1975.tb01405.x

Eaton, M. J. (2010). Dwarf crocodile *Osteolaemus tetraspis*. In S. C. Manolis, & C. Stevenson (Eds.), *Crocodiles: Status, Survey and Conservation Action Plan* (pp. 127–132). IUCN Crocodile Specialist Conservation Group.

Efron, B. (1979). Bootstrapping methods: Another look at the jackknife. *The Annals of Statistics*, 7(1), 1–26. doi:10.1214/aos/1176344552

Erickson, B. R. (1972). *Albertochampsa langstoni*, gen. et. sp. nov., a new alligator from the Cretaceous of Alberta. *Scientific Publications of the Science Museum of Minnesota*, 2(1), 1–13.

Erickson, B. R. (1976). Osteology of the Early Eusuchian Crocodile *Leidyosuchus formidabilis*, sp. nov. *The Science Museum of Minnesota Monograph: Paleontology*, 2, 1–61.

Estes, R. (1988). Lower vertebrates from the Golden Valley Formation, early Eocene of North Dakota (USA). *Acta Zoologica Cracoviensia*, 31(2), 11–27.

Felsenstein, J. (1985). Confidence limits on phylogenies: An approach using the bootstrap. *Evolution*, 39(4), 783–791. doi:10.2307/2408678

Frederick, P. C., & Collopy, M. W. (1989). The role of predation in determining reproductive success of colonially nesting wading birds in the Florida Everglades. *The Condor*, 91(4), 860–867. doi:10.2307/1368070

Gazin, C. L. (1962). A further study of the lower Eocene mammalian faunas of southwestern Wyoming. *Smithsonian Miscellaneous Collections*, 144(1), 1–98.

Gilmore, C. W. (1911). A new fossil alligator from the Hell Creek beds of Montana. *Proceedings of the United States National Museum*, 41(1860), 297–301. doi:10.5479/si.00963801.41-1860.297

Gmelin, J. F. (1789). *Caroli a Linné. Systema Naturae per Regna Tria Naturae, Secundum Classes, Ordines, Genera, Species, Cum Characteribus, Differentiis, Synonymis, Locis (Vol. 1, Ed. 13).* Impensis Georg. Emanuel. Beer.

Goloboff, P. A., Farris, J. S., Källersjö, M., Oxelman, B., Ramirez, M. J., & Szumik, C. A. (2003). Improvements to resampling measures of group support. *Cladistics*, 19(4), 324–332. doi:10.1111/j.1096-0031.2003.tb00376.x

Goloboff, P. A., Farris, J. S., & Nixon, K. C. (2008). TNT, a free program for phylogenetic analysis. *Cladistics*, 24(5), 774–786. doi:10.1111/j.1096-0031.2008.00217.x

Gray, J. E. (1844). *Catalogue of tortoises, crocodilians, and amphisbaenians in the collection of the British Museum*. Edward Newman.

Harrington, G. J., Clechenko, E. R., & Kelly, D. C. (2005). Palynology and organic–carbon isotope ratios across a terrestrial Palaeocene/Eocene boundary section in the Williston Basin, North Dakota, USA. *Palaeogeography, Palaeoclimatology, Palaeoecology*, 226(3–4), 214–232. doi:10.1016/j.palaeo.2005.05.013

Hastings, A. K., Reisser, M., & Scheyer, T. M. (2016). Character evolution and the origin of Caimaninae (Crocodylia) in the New World Tropics: new evidence from the Miocene of Panama and Venezuela. *Journal of Paleontology*, 90(2), 317–332. doi:10.1017/jpa.2016.37

Hickey, L. J. (1967). *The paleobotany and stratigraphy of the Golden Valley Formation in western North Dakota* [Unpublished doctoral dissertation]. Princeton University.

Hickey, L. J. (1977). Stratigraphy and paleobotany of the Golden Valley Formation (early Tertiary) of western North Dakota. *Geological Society of America*, 181.

Hutchinson, P. J., & Kues, B. S. (1985). Depositional environments and paleontology of Lewis Shale to lower Kirtland shale sequence (Upper Cretaceous), Bisti area, northwestern New Mexico. *New Mexico Bureau of Mines and Mineral Resources Circular*, 195, 25–54.

Janis, C. M., Scott, K. M., & Jacobs, L. (1998). *Evolution of Tertiary mammals of North America (Vol. 1)*. Cambridge University Press.

Janis, C. M., Gunnell, G. F., & Uhen, M. D. (2008). *Evolution of Tertiary mammals of North America (Vol 2)*. Cambridge University Press.

Jepsen, G. L. (1963). Eocene vertebrates, coprolites, and plants in the Golden Valley Formation of western North Dakota. *Geological Society of America Bulletin*, 74(6), 673–684. doi:10.1130/0016-7606(1963)74[673:EVCAPI]2.0.CO;2

Kälin, J. A. (1936). *Hispanochampsa mülleri* nov. gen. sp., ein neuer Crocodilide aus dem unteren Oligocaen von Tárrega (Catalonien). Nebst einem Beitrag von B–. Peyer (Zurich): Über die Compressionserscheinungen am Typusexemplar von *Hispanochampsa mülleri* Kälin. Birkhäuser. Abh. Schweizer. Palaeontol. Gesellschaft, 58, 1–40.

Kälin, J. A. (1955). Crocodilia. In J. Piveteau (Ed.), *Traité de Paléontologie (Vol. 5)* (pp. 695–784). Masson.

Keroher, G. C. (1966). *Lexicon of geologic names of the United States for 1936*–1960 (Report 1200; Bulletin). USGS Publications Warehouse.

Linnaeus, C. (1758). *Systema naturae per regna tria naturae, secundum classes, ordines, genera, species, cum characteribus, differentiis, synonymis, locis (Vol. 1)*. Stockholm, Sweden: Laurentius Salvius.

Lucas, S. G., & Sullivan, R. M. (2004). The taxonomic status of *Chrysochampsa*, an Eocene crocodylian from North Dakota, USA and the paleobiogeography of *Allognathosuchus. Neues Jahrbuch für Geologie und Paläontologie - Monatshefte*, 8(8), 461–472. doi:10.1127/njgpm/2004/2004/461

Maddison, W. P., & Maddison, D. R. (2023). Mesquite: a modular system for evolutionary analysis. Version 3.81. http://www.mesquiteproject.org.

Magnusson, W. E., & Lima, A. P. (1991). The ecology of a cryptic predator, *Paleosuchus tigonatus*, in a tropical rainforest. *Journal of Herpetology*, 25(1), 41–48. doi:10.2307/1564793

Magnusson, W. E., & Campos, Z. (2010). Cuvier's Smooth–fronted Caiman *Paleosuchus palpebrosus*. In S. C. Manolis, & C. Stevenson (Eds.), *Crocodiles: Status, Survey and Conservation Action Plan* (pp. 40–42). IUCN Crocodile Specialist Conservation Group.

Mannion, P. D., Benson, R. B., Carrano, M. T., Tennant, J. P., Judd, J., & Butler, R. J. (2015). Climate constrains the evolutionary history and biodiversity of crocodylians. *Nature Communications*, 6(1), 8438. doi:10.1038/ncomms9438

Markwick, P. J. (1998). Crocodilian diversity in space and time: the role of climate in paleoecology and its implication for understanding K/T

extinctions. *Paleobiology*, 24(4), 470–497. doi:10.1017/S009483730002011X

Martin, J. E., Smith, T., Lapparent de Broin, F., Escuillié, F., & Delfino, M. (2014). Late Palaeocene eusuchian remains from Mont de Berru, France, and the origin of the alligatoroid *Diplocynodon. Zoological Journal of the Linnean Society*, 172(4), 867–891. doi:10.1111/zoj.12195

McInerney, F. A., & Wing, S. L. (2011). The Paleocene–Eocene Thermal Maximum: A perturbation of carbon cycle, climate, and biosphere with implications for the future. *Annual Review of Earth and Planetary Sciences*, 39(1), 489–516. doi:10.1146/annurev-earth-040610-133431

McKenna, M. C. (1960). Fossil Mammalia from the early Wasatchian Four Mile Fauna, Eocene of north–west Colorado. *University of California Publications in Geological Sciences*, 37, 1–131.

Mendoza, M., Janis, C. M., & Palmqvist, P. (2005). Ecological patterns in the trophic–size structure of large mammal communities: a 'taxon–free' characterization. *Evolutionary Ecology Research*, 7(4), 505–530.

Mook, C. C. (1921). Allognathosuchus, a new genus of Eocene crocodilians. *Bulletin of the American Museum of Natural History*, 44, 105–110.

Mook, C. C. (1941). A new crocodilian, *Hassiacosuchus kayi*, from the Bridger Eocene beds of Wyoming. *Annals of the Carnegie Museum*, 28, 207–220. doi:10.5962/p.330789

Murphy, E. C. (2009). The Golden Valley Formation. *North Dakota Geological Survey DMR Newsletter*, 7, 1–4.

Murphy, E. C., Moxness, L. D., & Kruger, N. W. (2023). Elevated critical mineral concentrations associated with the Paleocene–Eocene Thermal Maximum, Golden Valley Formation, North Dakota. *Report of Investigation – North Dakota Geological Survey*, 133, 1–95.

Nagloo, N., Collin, S. P., Hemmi, J. M., & Hart, N. S. (2016). Spatial resolving power and spectral sensitivity of the saltwater crocodile, *Crocodylus porosus*, and the freshwater crocodile, *Crocodylus johnstoni. Journal of Experimental Biology*, 219(9), 1394–1404. doi:10.1242/jeb.135673

Nixon, K. C. (2002). *WinClada, version 1.00. 08*. Published by the author, Ithaca.

Norell, M. A., Clark, J. M., & Hutchison, J. H. (1994). The Late Cretaceous alligatoroid *Brachychampsa montana* (Crocodylia): new material and putative relationships. *American Museum Novitates*, 3116, 1–26.

Ouboter, P. E. (1996). *Ecological studies on crocodilians in Suriname: Niche segregation and competition in three predators*. SPB Academic Publishing.

Ouchley, K. (2013). *American Alligator: Ancient Predator in the Modern World*. University Press of Florida.

Pipiringos, G. N. (1955). Tertiary rocks in the central part of the Great Divide Basin, Sweetwater County, Wyoming. *Wyoming Geological Association 10th Annual Field Conference Guidebook* July 28–30, 1955. 100–104.

Platt, S., Rainwater, T., Finger, A., Thorbjarnarson, J., Anderson, T., & McMurry, S. (2006). Food habits, ontogenetic dietary partitioning and observations of foraging behaviour of Morelet's crocodile (*Crocodylus moreletii*) in Northern Belize. *The Herpetological Journal*, 16(3), 281–290.

Saalfeld, D. T., Conway, W. C., & Calkins, G. E. (2011). Food habits of American alligators (*Alligator mississippiensis*) in East Texas. *Southeastern Naturalist*, 10(4), 659–672. doi:10.1656/058.010.0406

Sasidhran, S., Adila, N., Hamdan, M. S., Samantha, L. D., Aziz, N., Kamarudin, N., Puan, C. L., Turner, E., & Azhar, B. (2016). Habitat occupancy patterns and activity rate of native mammals in tropical fragmented peat swamp reserves in Peninsular Malaysia. *Forest Ecology and Management*, 363, 140–148. doi:10.1016/j.foreco.2015.12.037

Scheyer, T. M., Aguilera, O. A., Delfino, M., Fortier, D. C., Carlini, A. A., Sánchez, R., Carrillo-Briceno, J. D., Quiroz, L., & Sánchez-Villagra, M. R. (2013). Crocodylian diversity peak and extinction in the late Cenozoic of the northern Neotropics. *Nature communications*, 4(1), 1907. doi:10.1038/ncomms2940

Scotese, C. R., Song, H., Mills, B. J., & van der Meer, D. G. (2021). Phanerozoic paleotemperatures: The earth's changing climate during the last 540 million years. *Earth–Science Reviews*, 215, 103503.

Shaney, K. J., Hamidy, A., Walsh, M., Arida, E., Arimbi, A., & Smith, E. N. (2017). Impacts of anthropogenic pressures on the contemporary biogeography of threatened crocodilians in Indonesia. *Oryx*, 53(3), 1–12.

Shirley, M. H., Vliet, K. A., Carr, A. N., & Austin, J. D. (2014). Rigorous approaches to species delimitation have significant implications for African crocodilian systematics and conservation. *Proceedings of the Royal Society B: Biological Sciences*, *281*(1776), 20132483. doi:10.1098/rspb.2013.2483

Shirley, M. H., Villanova, V. L., Vliet, K. A., & Austin, J. D. (2015). Genetic barcoding facilitates captive and wild management of three cryptic African crocodile species complexes. *Animal Conservation*, *18*(4), 322–330. doi:10.1111/acv.12176

Simpson, G. G. (1930). *Allognathosuchus mooki*, a new crocodile from the Puerco Formation. *American Museum Novitates*, *445*, 1–16.

Solórzano, A., Núñez-Flores, M., Inostroza-Michael, O., & Hernández, C. E. (2020). Biotic and abiotic factors driving the diversification dynamics of Crocodylia. *Palaeontology*, *63*(3), 415–429. doi:10.1111/pala.12459

Somaweera, R., Nifong, J., Rosenblatt, A., Brien, M. L., Combrink, X., Elsey, R. M., Grigg, G., Magnusson, W. E., Mazzotti, F. J., Pearcy, A., & Platt, S. G. (2020). The ecological importance of crocodylians: towards evidence-based justification for their conservation. *Biological Reviews*, *95*(4), 936–959. doi:10.1111/brv.12594

Staniewicz, A., Behler, N., Dharmasyah, S., & Jones, G. (2018). Niche partitioning between juvenile sympatric crocodilians in Mesangat Lake, East Kalimantan, Indonesia. *Raffles Bulletin of Zoology*, *66*, 528–537.

Stuebing, R. B., Bezuijen, M. R., Auliya, M., & Voris, H. K. (2006). The current and historic distribution of *Tomistoma schlegelii* (the False Gharial) (Müller, 1838) (Crocodylia, Reptilia). *Raffles Bulletin of Zoology*, *54*(1), 181–197.

Swofford, D. L. (2002). *PAUP*. Phylogenetic Analysis Using Parsimony (* and other methods). Version 4.0a169*. Sinaur Associates, Inc.

Tierney, J. E., Zhu, J., Li, M., Ridgwell, A., Hakim, G. J., Poulsen, C. J., Whiteford, R. D. M., Rae, J. W. B., & Kump, L. R. (2022). Spatial patterns of climate change across the Paleocene–Eocene Thermal Maximum. *Proceedings of the National Academy of Sciences*, *119*(42), e2205326119. doi:10.1073/pnas.2205326119

West, R. M. (1973). New Records of Fossil Mammals from the Early Eocene Golden Valley Formation, North Dakota. *Journal of Mammalogy*, *54*(3), 749–750. doi:10.2307/1378973

Western Regional Climate Center. (2016). Period of Record Monthly Climate Summary. Retrieved from https://wrcc.dri.edu/cgi–bin/cliMAIN.pl?nd2193.

Williamson, T. E. (1996). ?*Brachychampsa sealeyi*, sp nov.,(Crocodylia, Alligatoroidea) from the Upper Cretaceous (lower Campanian) Menefee Formation, northwestern New Mexico. *Journal of Vertebrate Paleontology*, *16*(3), 421–431. doi:10.1080/02724634.1996.10011331

Woodburne, M. O. (2004). *Late Cretaceous and Cenozoic mammals of North America: Biostratigraphy and geochronology*. Columbia University Press.

Woodburne, M. O., Gunnell, G. F., & Stucky, R. K. (2009). Climate directly influences Eocene mammal faunal dynamics in North America. *Proceedings of the National Academy of Sciences*, *106*(32), 13399–13403. doi:10.1073/pnas.0906802106

Wu, X. C., Brinkman, D. B., & Russell, A. P. (1996). A new alligator from the Upper Cretaceous of Canada and the relationship of early eusuchians. *Palaeontology*, *39*, 351–376.

Handling & Phylogenetics Editor: Pedro Godoy.